EXPLORING THE ORIGINS OF SECONDARY GROWTH – TWO LOWER DEVONIAN (EMSIAN) EUPHYLLOPHYTES FROM GASPE, CANADA, AND THEIR IMPLICATIONS FOR THE EVOLUTION OF SECONDARY GROWTH

By

Kelly C. Pfeiler

A Thesis Presented to

The Faculty of Humboldt State University

In Partial Fulfillment of the Requirements for the Degree

Master of Science in Biology

Committee Membership

Dr. Alexandru M.F. Tomescu, Committee Chair

Gar Rothwell, Committee Member

Paul Kenrick, Committee Member

Michael Mesler, Committee Member

Paul Bourdeau, Graduate Coordinator

May 2020

ABSTRACT

EXPLORING THE ORIGINS OF SECONDARY GROWTH – TWO LOWER DEVONIAN (EMSIAN) EUPHYLLOPHYTES FROM GASPE, CANADA, AND THEIR IMPLICATIONS FOR THE EVOLUTION OF SECONDARY GROWTH

Kelly C. Pfeiler

Secondary growth from a vascular cambium has a deep fossil record among euphyllophytes, with the earliest occurrence dated to 407 Ma. To date, *Armoricaphyton* and *Franhueberia* represent the only instances of secondary growth formally documented in the Early Devonian. Secondary growth diversified rapidly and was present in all major euphyllophyte lineages by the Middle Devonian. Here, I describe two new Early Devonian euphyllophytes exhibiting secondary growth, from the Emsian (c. 400-395 Ma) Battery Point Formation (Québec, Canada): G*mujij tetraxylopteroides* gen. et sp. nov. and *Perplexa praestigians* gen et sp. nov. Both these plants possess mesarch actinosteles with *Psilophyton*-type tracheid thickenings, and each represents a new type of anatomical organization among Early Devonian wood-producing euphyllophytes. These new Early Devonian plants reveal an unexpected level of diversity in the early stages of the first major tracheophyte radiation. Importantly, G*mujij* and *Perplexa*, together with the other Early Devonian euphyllophytes exhibiting secondary growth, reinforce existing hypotheses about the modular regulation of vascular cambial growth and demonstrate

that vascular cambial growth is an assemblage of regulatory modules whose deployment followed a mosaic pattern in the evolution of tracheophytes.

ACKNOWLEDGEMENTS

I thank the late Francis M. Hueber, who collected the specimens containing the new species presented here; William DiMichele, Carol Hotton, and Jonathan Wingerath (National Museum of Natural History – Smithsonian Institution) for facilitating specimen loans; Kelly K.S. Matsunaga (Chicago Botanic Garden/University of Kansas) for help during work in the NMNH collections; Marty Reed and David S. Baston (Bio Core Facility, Humboldt State University) for maintaining and providing access to microscopic imaging equipment; Michael Dunn (Cameron University) and Anne-Laure Decombeix (Université de Montpellier) for providing specimens and images for comparisons; Jaclyn Patmore and Justin Delgado for assistance with scanning electron microscopy and specimen preparation; and Matthew J. Reilly and Kevin Landaw for R guidance. The research has been supported by a Geological Society of America graduate student research grant to KCP. Initial assessment of the NMNH collection of Gaspé specimens was made possible by an American Philosophical Society grant to AMFT.

TABLE OF CONTENTS

Abstract ii

Acknowledgements iv

List of Figures viii

Chapter 1 viii

Chapter 2 viii

List of Tables x

Chapter 1 x

Chapter 2 x

Chapter 1: An Early Devonian actinostelic euphyllophyte with secondary growth from the Emsian of Gaspé (Canada) and the importance of tracheid wall thickening patterns in early euphyllophyte systematics 1

Introduction 1

Materials and Methods 4

Results 6

Systematics 6

Description 8

Comparisons 10

Discussion 11

Area of missing tissue 11

Rays 12

Comparison with Lower Devonian plants 13

Comparison with younger actinostelic plants 14

Comparisons based on xylem anatomy 15

Tracheid secondary wall thickenings 17

Conclusion 18

References 21

Figures 25

Appendix 35

Chapter 2: Mosaic assembly of regulatory programs for vascular cambial growth: a view from the Early Devonian 39

Introduction 39

Materials and Methods 41

Results 43

Systematics 43

Description 45

Comparisons 51

Discussion 53

The primary body of *Perplexa* 53

Taxonomy 54

Secondary xylem recognition 56

The mode of secondary growth of *Perplexa praestigians* 57

Radial tissue systems and synchronization of periclinal divisions in Early Devonian euphyllophytes 59

Mosaic deployment of regulatory modules for secondary growth in Early Devonian euphyllophytes 60

Conclusion 64

References 66

Tables 71

Figures 74

LIST OF FIGURES

Chapter 1

Figure 1. ***Gmujij tetraxylopteroides*** **gen. & sp. nov.** xylem anatomy. 25

Figure 2. ***Gmujij tetraxylopteroides*** **gen. & sp. nov.** tracheid pitting and rays. 27

Figure 3. ***Gmujij tetraxylopteroides*** **gen. & sp. nov.** tracheid anatomy (scanning electron micrographs of longitudinal sections). 28

Figure 4. ***Gmujij tetraxylopteroides*** **gen. & sp. nov.** tracheid anatomy (scanning electron micrographs of longitudinal sections). 29

Figure 5. Comparisons of metaxylem and secondary xylem tracheid width. 30

Figure 6. Comparisons of metaxylem and secondary xylem tracheid width and tracheid cross-sectional lumen area. 31

Figure 7. Comparisons of secondary xylem tracheid width, measured in files from the areas around the tips of primary xylem lobes and in files from areas of the embayments between the lobes. 32

Figure 8. Comparisons of secondary xylem tracheid width and tracheid cross-sectional lumen area, measured in files from the areas around the tips of primary xylem lobes.. .. 33

Chapter 2

Figure 1. ***Perplexa praestigians*** **gen. et sp. nov.** axis anatomy in cross section..... 74

Figure 2. ***Perplexa praestigians*** **gen. et sp. nov.** xylem anatomy in cross section from the basal portion to the distal portion of the axis. 76

Figure 3. ***Perplexa praestigians*** **gen. et sp. nov.** anatomical variation along the axis. . 78

Figure 4. ***Perplexa praestigians*** **gen. et sp. nov.** epidermis and sclerified outer cortex in cross section. 80

Figure 5. ***Perplexa praestigians* gen. et sp. nov.** longitudinal sections of sclerified outer cortex and inner cortical cells in longitudinal section. 81

Figure 6. ***Perplexa praestigians* gen. et sp. nov**. multiplicative divisions in the secondary xylem. 83

Figure 7. ***Perplexa praestigians* gen. et sp. nov.** radial component of secondary xylem. 84

Figure 8. ***Perplexa praestigians* gen. et sp. nov.** primary xylem anatomy in longitudinal section. 86

Figure 9. ***Perplexa praestigians* gen. et sp. nov.** longitudinal views of tracheid anatomy in scanning electron microscopy..... 88

Figure 10. Comparisons of metaxylem and secondary xylem tracheid widths. 90

Figure 11. Comparisons of roundness and circularity of metaxylem tracheids..... 91

LIST OF TABLES

Chapter 1

Table 1. Summary statistics for comparisons between metaxylem and secondary xylem tracheid sizes. 35

Table 2. Summary statistics for comparisons of sizes of secondary xylem tracheids that are located in either the areas around the tips of primary xylem lobes (lobe) or the areas in the embayments between lobes (bay). 37

Chapter 2

Table 1. Summary statistics for comparisons of metaxylem tracheid widths (µm)..... 71

Table 2. Summary statistics for comparisons of secondary xylem tracheid radial and tangential widths (µm). 72

Table 3. Mosaic expression of anatomical fingerprints and corresponding developmental processes or hypothesized regulatory modules controlling vascular cambial growth in Early Devonian euphyllophytes. 73

CHAPTER 1: AN EARLY DEVONIAN ACTINOSTELIC EUPHYLLOPHYTE WITH SECONDARY GROWTH FROM THE EMSIAN OF GASPÉ (CANADA) AND THE IMPORTANCE OF TRACHEID WALL THICKENING PATTERNS IN EARLY EUPHYLLOPHYTE SYSTEMATICS

Introduction

Secondary growth is responsible for the production of secondary xylem (wood) and represents a major structural innovation of plants with a deep fossil record (Groover & Spicer 2010; Gerrienne *et al.* 2011). In fossils, secondary growth is identified using a clear set of anatomical criteria: radially aligned cell files (seen in cross sections), anticlinal divisions leading to addition of new such files, and organization that includes an axial (e.g. tracheary elements) and a radial component (rays) (Hoffman & Tomescu 2013).

Today, secondary growth is present in the two major tracheophyte clades – in the seed plants, among euphyllophytes, and in the isoetaleans, among lycophytes (Decombeix *et al.* 2019). In contrast to the extant flora, the fossil record shows a high diversity of lineages with secondary vascular tissues, which are recorded in both of the major tracheophyte clades by the Carboniferous (ca. 350 Ma ago). Deeper in the fossil record, euphyllophytes exhibiting secondary growth can be traced to the Middle-Late Devonian (390-360 Ma) and are placed in several well-circumscribed groups: cladoxylopsids, sphenophytes, rhacophytaleans, zygopterids, progymnosperms,

stenokolealeans, and seed plants (Cichan & Taylor 1990). Until recently, the lack of fossil plants with secondary growth older than these Middle-Late Devonian occurrences has informed the traditional hypothesis that secondary growth evolved independently in each of these major groups (Groover & Spicer 2010).

Discovery of a handful of notable fossils with secondary growth has pushed the origin of this feature deeper in time, into the Early Devonian. *Armoricaphyton chateaupannense*, a euphyllophyte from the late Pragian-early Emsian (c. 407 Ma), represents the earliest documented occurrence of secondary growth in the fossil record (Gerrienne *et al.* 2011; Strullu-Derrien *et al.* 2014). Two younger euphyllophytes with secondary growth have been reported from the Emsian of eastern Canada: *Franhueberia gerriennei* (Hoffman & Tomescu 2013) and a plant initially reported by Gerrienne *et al.* (2011) and currently referred to as New Brunswick plant A (Gensel 2018). These three plants represent two types of anatomical organization. *Armoricaphyton* and *Franhueberia* are characterized by terete centrarch protosteles with *Psilophyton*-type (P-type) tracheid thickenings. New Brunswick plant A also has P-type tracheid thickenings but differs in having an oval protostele with elongate central protoxylem. These early occurrences of secondary growth are approaching the age of the euphyllophyte clade as a whole – c. 425 Ma (based on the earliest known occurrences of the euphyllophyte sister group, the zosterophylls; (Kotyk *et al*. 2002). This raises the possibility that secondary growth, or at least some of the major pathways responsible for its regulation, may have a single origin in an ancestral euphyllophyte (Hoffman & Tomescu 2013; Tomescu &

Groover 2019), thus challenging traditional hypotheses on the origins of secondary growth.

The anatomical simplicity and the fragmented nature of these Early Devonian fossils prevent us from classifying these plants into any of the previously circumscribed, younger taxonomic groups. This is because characters traditionally used to distinguish Middle-Late Devonian euphyllophyte lineages prove inadequate for these anatomically simple Early Devonian plants with secondary growth. These characters include branching patterns, sporangial features and anatomical features, many of which are missing in the Early Devonian fossils. Furthermore, comparative studies of the anatomy of secondary growth in each euphyllophyte lineage show that many anatomical characters of secondary tissues are shared among lineages (Cichan & Taylor 1990) and few of them have diagnostic value. These considerations emphasize the need for detailed reassessment of the comparative anatomy of primary and secondary growth, aimed at identifying additional characters for more conclusive comparisons and better resolved classification of Early Devonian plants.

Here I describe a new Emsian plant with a type of anatomical organization previously unknown among the wood-bearing euphyllophytes of the Early Devonian. This plant, characterized by a four lobed mesarch actinostele, adds to the growing anatomical diversity of Early Devonian euphyllophytes exhibiting secondary growth. In characterizing this plant, I introduce and employ additional anatomical characters that can be used to describe variation and draw comparisons among the anatomically simple Early Devonian plants.

Materials and Methods

The specimen described here is preserved by cellular permineralization with calcium carbonate in a cobble collected by Dr. Francis M. Heuber (Smithsonian Institution – U.S. National Museum of Natural History) in 1965 from an exposure of the Battery Point Formation on the south shore of Gaspé Bay, near Douglastown, Québec, Canada. The allochthonous assemblages that host this and other permineralized fossil plants are late Emsian in age, ca. 402-394 Ma old, and are part of sediments deposited in braided fluvial to coastal environments (Cant & Walker 1976; Griffing *et al.* 2000).

Serial anatomical sections were obtained using the cellulose acetate peel technique (Joy *et al.* 1956). Sections for bright field microscopy were mounted with Eukitt (O. Kindler, Freiburg, Germany). Images were captured using a Nikon Coolpix 8800VR digital camera mounted on a Nikon E400 compound microscope and an Olympus Dp73 digital camera mounted on an Olympus SZX16 microscope. Scanning electron micrographs were generated using a FEI Quanta 250 (Hillsboro, Oregon, USA) from cellulose acetate peels prepared using the method detailed in Matsunaga *et al.* (2013). Images were processed using Adobe Photoshop (San Jose, California, USA).

Tracheid size measurements were performed in ImageJ (US National Institutes of Health; https://imagej.nih.gov/ij) directly on slides of fossil material for *Gmujij*, the early spermatophytes *Tetrastichia* (CUPH 712-1-5 Atop #182; courtesy of Michael T. Dunn), and *Triradioxylon* (CUPH 712-1-18 Bbot #22; courtesy of Michael T. Dunn); the *Triradioxylon* specimen used for measurements was originally identified and figured by

Dunn & Rothwell (2012) as *Tetrastichia* (M.T. Dunn, pers. comm. 2019). For the progymnosperm *Tetraxylopteris*, measurements were performed on a photograph of ULg 4418-obj32V2 (courtesy of Anne-Laure Decombeix). For *Gmujij*, measurements were performed in multiple sections over c. 1 mm of axis length. In all these plants I measured the largest well preserved tracheids in the areas of the axis that were least disturbed by taphonomic processes (e.g., Fig. 1D, E). For each tracheid I measured the radial and tangential width. Radial tracheid sizes in the metaxylem were measured in directions perpendicular to the mid-planes of xylem lobes; tangential sizes were measured parallel to the mid-planes. In the secondary xylem I selected well preserved radial tracheid files within which all tracheids were measured. Radial files of secondary xylem tracheids were measured from either the areas around the tips of primary xylem lobes (lobe files) or the areas in the embayments between lobes (bay files). In both the metaxylem and the secondary xylem, I took special care to avoid measuring tracheids that exhibited any signs of potential taphonomic distortion. The cross-sectional surface area (lumen area) of tracheids was approximated by multiplying the tangential width by the radial width of each tracheid. Summary statistics of measurements and box plots were obtained using Microsoft Excel; I made the scatterplots with ggplot in R (R Core Team 2018). All measurement data used in comparisons are deposited as supplemental data hosted on the Theses and Projects web page (Digital Commons, Humboldt State University, Arcata, California; https://digitalcommons.humboldt.edu/etd/). Cobble slabs, acetate peels, slides, and SEM stubs are stored at the Smithsonian Institution – U.S. National Museum of Natural History under collection number USNM 557840.

Institutional abbreviations. CUPH, Cameron University Paleobotanical Herbarium, Lawton, OK, USA – specimens to be transferred to the National Museum of Scotland, Edinburgh, UK; ULg, Department of Geology, University of Liège, Belgium; USNM, National Museum of Natural History – Smithsonian Institution, Washington, D.C., USA.

Results

Systematics

Division: Tracheophyta Cavalier-Smith, 1998

Subdivision: Euphyllophytina Kenrick & Crane, 1997

Infradivision: Radiatopses Kenrick & Crane, 1997

Gmujij Pfeiler et Tomescu gen. nov.

Generic diagnosis: Small axes with four-lobed primary xylem and secondary xylem. Primary xylem maturation mesarch, with several protoxylem strands along midplanes of xylem lobes and one central protoxylem strand. Primary and secondary xylem tracheids with *Psilophyton*-type secondary wall thickenings. Multiplicative divisions and rays present in secondary xylem.

Etymology: G*mujij* is derived from the Mi'gmaq words for “small stick” (gmu'ji'j) (https://www.mikmaqonline.org; accessed 23 October 2019). The Mi'gmaq are the indigenous population of parts of eastern Canada, including the Gaspé Peninsula.

Gmujij tetraxylopteroides Pfeiler et Tomescu sp. nov.

Specific diagnosis: Xylem diameter 1.4-2 mm and primary xylem ca. 1 mm in diameter. Primary xylem lobes ca. 0.5 mm long in cross sections of axes. Metaxylem tracheids 26-48 µm in radial diameter and 15-42 µm in tangential diameter. Aperture membranes of *Psilophyton*-type tracheid thickenings in metaxylem up to 23.5 µm in height, with multiple round apertures 6.7 µm in diameter. Secondary xylem tracheids measure 12-32 µm tangentially and 16-48 µm radially. P-type pitting present on both radial and tangential walls of secondary xylem tracheids. Aperture membranes of P-type thickenings up to 17 µm in height, horizontal thickenings up to 16 µm wide, and pit apertures as wide as 8.7 µm. Rays ca. 30 µm wide, some of them continuous throughout the thickness of secondary xylem while others are terminated abruptly at the peripheral end by a file of tracheids.

Etymology: *tetraxylopteroides* refers to the anatomical similarity of this plant to the aneurophyte progymnosperm *Tetraxylopteris*.

Holotype: Axis in USNM 557840, slabs G and F (slides Gbot series c, Gtop series d, G side (2), and Fbot series e).

Paratype: Axis in USNM 557840, slabs H and I (slides Hbot series f and Itop series a).

Locality and horizon: Battery Point Formation, in the vicinity of Douglastown, south shore of Gaspé Bay (Quebec, Canada); mid- to late Emsian (Early Devonian; McGregor 1977; Hoffman & Tomescu 2013), c. 400–395 Ma.

Description

Gmujij tetraxylopteroides is represented by one unbranched fragment of a decorticated axis (Fig. 1A, B) that is more than 19 mm in length and another decorticated charcoalified axis fragment (Fig. 1C) more than 6.8 mm in length. Primary phloem and cortical tissues are not preserved. These axes have four-lobed central primary xylem and small amounts of secondary xylem. The overall diameter of the xylem ranges from 1.4-2 mm (the largest diameter measured where the axis was compressed in an oblique angle).

The central primary xylem consists of a cruciform actinostele. Parts of the primary xylem are missing in various amounts along the central region of the non-charcoalified specimen (Fig. 1C), likely as a result of detritivory (see discussion). The primary xylem, 1.06 mm in maximum diameter (measured between the ends of two opposite lobes) has relatively short lobes, 0.53 mm in length. Crushed cells with poor preservation form dark lines along the mid-plane of the lobes (Fig. 1A). Based on the position of these crushed cells, as well as on the presence of smaller metaxylem tracheids at several points adjacent to the lobe mid-planes, I infer that protoxylem strands were present along primary xylem lobes, consistent with mesarch xylem maturation. The charcoalified specimen also exhibits areas of small crushed cells, interpreted as putative protoxylem strands, at the center and along the mid-planes of primary xylem lobes (Fig

1C). Metaxylem tracheids are elongated in directions perpendicular to the mid-planes of xylem lobes (radially heretofore), 26-48 x 15-42 µm in diameter (Figs 1D, 5, 6A, B; Appendix). The walls of metaxylem tracheids are up to 12 µm thick and have P-type thickenings (Figs 2A, 3A). Thickenings are up to 23.5 µm in height. Apertures are round and the largest measure 6.7 µm (Figs 3C, D, 4A).

The boundary between metaxylem and secondary xylem is inconspicuous, marked only by the presence of radially aligned tracheids (Figs 1A, D, E). Tracheids in the secondary xylem are rectangular in cross section (Fig 1D), and measure 12-32 µm tangentially and 16-48 µm radially (Fig 6A, B; Appendix). The walls of secondary xylem tracheids are thinner (up to 6 µm) than those in the primary xylem. Thickness of the secondary xylem varies slightly around the periphery of the primary xylem. It is thicker in the bays between primary xylem lobes (0.32 mm) than around the lobe tips (0.24 mm). This difference is also expressed in correspondingly higher (up to 13 in bays) and lower (7-9 around lobe tips) numbers of cells per radial tracheid file, as well as in the sizes of secondary xylem tracheids, which are smaller around the primary xylem lobes than in the bays (Figs 7, 8A, B). Secondary xylem tracheids have P-type pitting on both radial and tangential walls. Pits measure 9-17 µm in height and pit aperatures are circular are up to 8.7 µm in diameter. Thickenings are 2-16 µm thick. (Fig 2B, 3B, 4B, C). Multiplicative divisions (Fig 2D) are scant (1-3 divisions observed per cross section) and may happen as close to the primary xylem as the 3rd cambial division.

In the secondary xylem there are areas where two adjacent tracheid files have been split apart due to taphonomic factors, leaving an open space (Fig 2C). In other

areas, I observe individual tracheid files that terminate abruptly, leaving an empty space between the neighboring tracheid files that continue alongside the empty space (Fig 2D). In some cases, such empty spaces are enclosed at the distal end by a file of tracheids (Fig 2E). Whether open or closed, these spaces with missing tracheids are surrounded only by the walls of neighboring tracheids (Fig 2C, D, E). These structures are up to 30 µm in width and their position and length vary. They are found in numbers as high as four per cross section and I interpret them as rays in which parenchymatous cells have not been preserved (see discussion).

Comparisons

In comparisons of tracheid size between *Gmujij*, *Tetraxylopteris*, *Tetrastichia* and *Triradioxylon*, secondary xylem tracheids are smaller, overall, than the metaxylem tracheids in both tangential and radial dimension, in all four plants (Figs 5, 6A, B; Appendix). However, the difference between secondary xylem and metaxylem tracheids is minimal in *Tetraxylopteris* and *Gmujij*, whereas in *Triradioxylon* and especially *Tetrastichia* metaxylem tracheids are much larger than secondary xylem tracheids. The same trends are reflected in the cross-sectional area of tracheids (Fig 6C; Appendix). The size of metaxylem tracheids varies more broadly between the four plants, whereas secondary xylem tracheids show small differences (ca. 23-36 µm averages, including both tangential and radial sizes).

In the secondary xylem, tracheids of the lobe files have smaller tangential size than those of bay files, in *Tetrastichia*, *Triradioxylon*, and *Tetraxylopteris* (Figs 7, 8A, B;

Appendix). In *Gmujij*, the tangential sizes of lobe and bay tracheids have overlapping ranges (Figs 7, 8). Radial tracheid sizes show different patterns in each plant. Their ranges overlap in *Gmujij* and Tetrastichia, but in *Tetraxylopteris* bay tracheids have larger radial sizes than lobe tracheids and in *Triradioxylon* the pattern is reversed, bay tracheids are smaller in radial size that lobe tracheids (Figs 7, 8). The cross-sectional surface area of tracheids (Fig 8C) shows differences between lobe and bay tracheids similar to those of the radial tracheid dimensions, except for *Tetrastichia*, in which bay tracheids are larger than lobe tracheids (like in *Tetraxylopteris*).

Discussion

Area of missing tissue

Gmujij tetraxylopteroides is represented solely by fragments of xylem strands. The axes likely lost extraxylary tissues during transport and deposition. The central area of missing tissue (Fig 1A) is wide at one end, where it fragments the axis, whose tissues are also highly distorted, and tapers to 0.3 mm in diameter over the 3.85 mm of axis length that was exposed in serial cross sections. The cause for the missing tissue is unclear, but the random shape of the gap and its location slightly off-center and cutting through tissues indiscriminately, preclude interpretation as a central parenchymatous pith-like area that may have been lost to differential preservation. Furthermore, the charcoalified specimen does not have such a central area of missing tissue. The clear-cut edges of this area of missing tissue rule out microbial or fungal decomposition, which tends to be more

diffuse. This leaves as probable causes herbivory or detritivory, which can be hard to tease apart. Given that arthropods capable of consuming xylem (such as oribatid mites) are not known in the Early Devonian, and that the specimen shows no evidence of faecal pellets, the most probable explanation is that the missing tissue was removed by a burrowing detritivore.

Rays

The ray-like spaces observed along tracheid files within the secondary xylem differ conspicuously from taphonomic tears between tracheid files in the secondary xylem (compare Fig 2C and Fig 2D, E). These spaces have consistently the thickness of one tracheid file and some are confined by tracheids at both ends. Consequently, they represent the location of missing cells that cannot be explained by fortuitous non-preservation of tracheids. They are best interpreted as the locations of parenchymatous cells that were not preserved given harsh taphonomic factors (which also obliterated the extra-xylary tissues). The geometry and location of these parenchymatous cells are similar to those interpreted as rays in *Armoricaphyton* (Gerrienne *et al.* 2011). Consistent with this interpretation, the rays of *G. tetraxylopteroides* are surrounded only by the secondary walls of the adjacent tracheids (Gerrienne *et al.* 2011; Hoffman & Tomescu 2013).

Comparison with Lower Devonian plants

Aside from *Gmujij tetraxylopteroides*, other Early Devonian plants with lobed primary xylem include *Gothanophyton zimmermanni* (Remy & Hass 1986), *Leptocentroxyla tetrarcha* (Bickner & Tomescu 2019), an unnamed euphyllophyte described by (Gensel 1984) from the Battery Point Formation, and another plant described from the same unit by Toledo (2018); see also Kenrick & Crane 1997, fig. 4.24.a). Toledo's plant is larger than *Gmujij*, with larger primary xylem (c. 5 mm), larger metaxylem tracheids, and secondary xylem tracheids twice the size of those of *Gmujij*. Gensel's plant differs from the new plant by having larger, three-lobed primary xylem consisting of tracheids with scalariform thickenings or oval to circular pits (as reported by Gensel 1984, p. 785; although one of the anonymous reviewers of this paper has noted that the pitting pattern in that plant is P-type). *Gothanophyton* has lateral xylem traces that are somewhat comparable (1.7 mm wide) to *Gmujij*. However, the primary xylem of both the main axis and the laterals of *Gothanophyton* is 4-6-lobed and consists of metaxylem tracheids that are more than double the size of those of *Gmujij*. Moreover, *Gothanophyton* possesses tracheids with scalariform to reticulate pitted walls. Finally, *Leptocentroxyla* has a primary xylem strand that is the same diameter as *Gmujij* (~1.1 mm), however the diameter of metaxylem tracheids of this new plant is smaller than those of *Leptocentroxyla*. More generally, with the exception of Toledo's plant, these Early Devonian plants have not been demonstrated to possess secondary growth.

Comparison with younger actinostelic plants

The mesarch primary xylem maturation and the protoxylem architecture that I infer for *Gmujij*, with protoxylem strands located centrally and along xylem lobe midplanes, are consistent with radiatopsid affinities. Several actinostelic radiatopsid euphyllophytes spanning the Late Devonian to lower Mississippian interval are similar to *Gmujij*. Among these, the most closely comparable are the progymnosperm *Tetraxylopteris* (Frasnian) and the early seed plants *Triradioxylon* (Tournaisian) and *Tetrastichia* (Tournaisian) (Beck 1957; Matten & Banks 1967; Dunn & Rothwell 2012). All three are (or can be – *Triradioxylon*) characterized by four-lobed primary xylem, secondary growth, and possess tracheids with bordered pits. Whereas the *Triradioxylon* specimen I used in comparisons is similar in size to *Gmujij*, both *Tetraxylopteris* and *Tetrastichia* have larger axes.

Comparisons based on tracheid sizes reveal that all four genera have metaxylem tracheids larger than secondary xylem tracheids, although the magnitude of this disparity is different in each genus (Figs 5, 6; Appendix). In contrast to this pattern, the differences seen between lobe and bay file tracheids in the secondary xylem do not show the same trend in each of the four genera. Instead, these differences distinguish the four genera (Figs 7, 8). These results indicate that a numerical comparative approach to tracheid size distributions has potential for taxonomic differentiation that needs to be explored further. These comparisons also indicate that *Gmujij* is most similar to *Tetraxylopteris* in the small size difference between metaxylem and secondary tracheids

(Fig 6), but it differs from the latter in the comparative size of bay and lobe tracheids (Fig 8).

Comparisons based on xylem anatomy

It would be interesting to know to what extent the differences in xylem anatomy I observed between the taxa compared here, reflect functional features or taxonomic signals. To our knowledge, neither of the two types of comparisons – (1) tracheid sizes in primary xylem (metaxylem) vs secondary xylem, and (2) tracheid sizes in lobe vs bay tracheids of the secondary xylem – have been previously explored in fossil or extant plants, let alone specifically in plants with comparable protostelic (actinostelic) xylem anatomy and small amounts of wood. In the absence of more comprehensive datasets, expanded discussions of functional or taxonomic nature can hardly raise above the level of mere speculation. Nevertheless, I report the results of my exploratory morphometric comparisons (Appendix, supplementary data 1) hoping they will serve as an example and baseline for future studies that may expand their scope.

Future studies expanding these datasets may either reinforce or dampen the apparent taxonomic signals carried by the morphometric differences I documented – such as the lumens of metaxylem tracheids in the early seed plants *Triradioxylon* and *Tetrastichia*, which are significantly larger than the secondary xylem in these plants, and also than either the primary or secondary xylem of *Gmujij* and the progymnosperm *Tetraxylopteris* (Fig 6). A cursory survey of the published literature reveals that protostelic plant axes with small amounts of wood run the whole gamut of ratios in terms

of metaxylem vs secondary xylem tracheid sizes. Thus, metaxylem tracheids are smaller than the secondary xylem in *Armoricaphyton*, *Franhueberia*, *Zygopteris*, and some calamitaceae, as well as in small roots glossopterids (*Vertebraria*) and extant *Pinus*; the opposite relationship is seen in the early sphenopsid *Rotafolia* and in many early (actinostelic) seed plants; finally, *Rhacophyton*, *Sphenophyllum*, stenokolealeans, and most aneurophyte progymnosperms have relatively equal-sized metaxylem and secondary xylem tracheids. Robust quantitative datasets that thoroughly sample tracheid morphometrics of all these taxa will be required to test whether these quick qualitative observations hold true.

Developmentally, the absolute and relative (as compared to metaxylem) sizes of secondary xylem tracheids reflect the absolute and relative sizes of cambial initials, another aspect of comparative anatomy never explored previously, to our knowledge, in either a taxonomic or a functional framework. Along the same lines, tracheid size disparities in different sectors of the secondary xylem of actinostelic axes may be related to physical constraints – such as the mechanics of cell packing in inter-lobe (bay) vs lobe tip regions – or may carry a taxonomic signal. At first glance, if mechanical constraints of cell packing cause significant size differences between inter-lobe and lobe area tracheids, we would expect to see consistently two clusters in the graphs (Fig 7) across all the taxa surveyed. Whereas the *Tetraxylopteris* and *Tetrastichia* graphs show some clustering consistent with this prediction, with inter-lobe tracheids slightly larger than those in the lobe areas, *Gmujij* shows no such clustering, suggesting that this type of morphometric data may also carry a taxonomic signal. Exploration of this and similar

questions in the future, with more extensive datasets that cover broader swaths of evolutionary time and taxonomic space, is bound to reveal interesting patterns and fuel meaningful discussions of function vs inheritance in xylem anatomy.

Tracheid secondary wall thickenings

All of the younger plants discussed above differ from *Gmujij* in lacking P-type tracheid pitting. The P-type pitting seen in Early Devonian plants is considered plesiomorphic among euphyllophytes and plants with this type of pitting are difficult to place into the well recognized groups of the Middle and Late Devonian, which have different tracheid pitting patterns. Currently, it is not known whether the evolutionary transition from P-type pitting to tracheids with bordered pits involved simple (and, therefore, likely) or complex changes in the regulatory mechanisms controlling secondary wall thickening patterns. If anything, the variety of thickening patterns present even within a single plant (e.g., between protoxylem, metaxylem, and secondary xylem tracheids, or between vessels, tracheids, and fibers) suggests that transitions between very different patterns require minor changes in regulation. Case in point, among Early Devonian fossils, another wood-producing plant from the Battery Point Formation, *Franhueberia*, possesses secondary xylem tracheids with typical P-type thickenings, and metaxylem tracheids that exhibit a range of thickening patterns, from P-type to separate round to oval bordered pits (Hoffman & Tomescu 2013). In an even more dramatic example, a putative zosterophyll from the Lower Devonian of Norway documented by Edwards *et al.* (2006) shows a transition between characteristic G-type tracheids and tracheids with bordered

pits between axes of different order of a single specimen, consistent with ideas that transitions between different pitting patterns occur readily and require minor changes in regulation.

If switches between secondary wall thickening patterns involve minor changes in regulatory mechanisms and occur frequently in the development of a plant, then tracheid pitting patterns may not carry enough weight in taxonomic decisions, such as exclusion of a fossil from a given taxonomic group based solely or primarily on tracheid pitting. If we take this view, then the similarity between *Gmujij* and *Tetraxylopteris* suggests that the former could represent an early progymnosperm. However, short of extensive knowledge on the morphology of the plant (e.g., branching patterns, types of appendages) and reproductive structures, more accurate and conclusive comparisons of vegetative anatomy are needed. Such comparisons would require improved knowledge of the anatomy of *Gmujij* (e.g., data on extraxylary tissues, anatomy of trace emission), as well as in-depth understanding of the regulatory programs responsible for tracheid wall thickening patterns and their variation.

Conclusion

Gmujij tetraxylopteroides adds to the growing diversity of anatomically preserved plants described from the Battery Point Formation. With its four-lobed actinostele, this plant exhibits anatomical similarities with younger (Middle-Late Devonian) euphyllophytes, especially aneurophytalean progymnosperms. However, understanding the taxonomic

affinities of Early Devonian euphyllophytes like *Gmujij* is complicated by the fact that (1) these plants are anatomically simple, in general; and (2) characters that have traditionally been used to compare Devonian euphyllophytes – such as branching architecture, the vascularization of appendages, and the anatomy of trace divergence to appendages – are incompletely preserved or unknown in these early representatives of the clade. Detailed documentation of such characters would also allow for exploration of the taxonomic placement of Early Devonian fossils in a phylogenetic context (e.g., Kenrick & Crane 1997; Toledo *et al.* 2018). In the absence of taxonomic and phylogenetic resolution on these plants it is difficult to utilize them in addressing the evolutionary origins of Late Devonian euphyllophyte groups, as well as the evolution of anatomy in this clade.

To further complicate matters, many Early Devonian plants, including *Gmujij*, possess P-type tracheid thickenings. Despite the fact that these plants exhibit clear anatomical similarities with younger Devonian euphyllophytes, their P-type thickenings draw a sharp line of separation from those younger groups, precluding conclusive taxonomic placement (Bickner & Tomescu 2019). The P-type secondary wall thickening pattern is considered plesiomorphic among euphyllophytes and it is currently unknown whether the evolutionary transition from P-type thickenings to tracheids with bordered pits involved simple or complex changes in the regulatory mechanisms controlling secondary wall thickening patterns. In-depth knowledge of regulatory programs responsible for tracheid pitting patterns and their variation is needed to understand how

informative P-type thickenings are as a diagnostic character separating major euphyllophyte lineages.

If we are to elucidate the relationships of the Early Devonian euphyllophytes, it will be necessary to (1) explore the molecular mechanisms that control distinct developmental components of secondary growth (Tomescu & Groover 2019), and (2) to develop more detailed characters for anatomical comparisons. Some of these characters may come from understanding of the regulation of secondary growth as a modular assemblage of processes, but it may also prove fruitful to use anatomical characters not considered previously in addressing taxonomic questions, like the ones I introduce and employ in this study. For example, the tracheid size distribution approach I used to draw comparisons between *Gmujij* and other coeval and younger plants shows its similarity to Middle Devonian radiatopsids, specifically the aneurophyte progymnosperm *Tetrastichia*. Documenting tracheid size distributions in other plants may prove useful for the inclusion of the anatomically simple Early Devonian plants into comparative studies that can provide clues about their relationships. With improved understanding of the developmental underpinnings of vascular anatomy, along with use of new characters to better describe anatomical variation in Early Devonian taxa, plants such as *Gmujij* could provide important insights into the evolution of secondary growth and the radiation in plant anatomical complexity that occurred during the Early Devonian.

References

BECK, C. B. 1957. *Tetraxylopteris schmidtii* gen. et sp. nov., a probable pteridosperm precursor from the Devonian of New York. *American Journal of Botany*, **44**, 350–367.

BICKNER, M. A. and TOMESCU, A. M. F. 2019. Structurally complex, yet anatomically plesiomorphic: permineralized plants from the Emsian of Gaspé (Quebec, Canada) expand the diversity of Early Devonian euphyllophytes. *IAWA Journal*, **40**, 421–445.

CANT, D. J. and WALKER, R. G. 1976. Development of a braided-fluvial facies model for the Devonian Battery Point Sandstone, Québec. *Canadian Journal of Earth Sciences*, **13**, 102–119.

CAVALIER-SMITH, T. 1998. A revised six-kingdom system of life. *Biological Reviews*, **73**, 203–266.

CICHAN, M. A. and TAYLOR, T. N. 1990. Evolution of cambium in geologic time - a reappraisal.pdf. *In* IQBAL, M. (ed.) *The vascular cambium*, Research Studies Press Ltd., Somerset, England, 213–229 pp.

DECOMBEIX, A.-L., BOURA, A. and TOMESCU, A. M. F. 2019. Plant hydraulic architecture through time: lessons and questions on the evolution of vascular systems. *IAWA Journal*, 1–34.

DUNN, M. T. and ROTHWELL, G. W. 2012. Phenotypic plasticity of the hydrasperman seed fern *Tetrastichia bupatides* Gordon (Lyginopteridaceae). *International Journal*

of Plant Sciences, **173**, 823–834.

EDWARDS , D., LI, C.-S. and RAVEN, J. A. 2006. Tracheids in an early vascular plant: A tale of two branches. *Botanical Journal of the Linnean Society*, **150**, 115–130.

GENSEL, P. G. 1984. A new Lower Devonian plant and the early evolution of leaves. *Nature*, **309**, 785–787.

———. 2018. Early Devonian woody plants and implications for the early evolution of vascular cambia. *In* KRINGS, M., HARPER, C., CUNEO, N. R. and ROTHWELL, G. W. (eds.) *Transformative paleobotany*, Vol. 1. Academic Press, London, 21–33 pp.

GERRIENNE, P., GENSEL, P. G., STRULLU-DERRIEN, C., LARDEUX, H., STEEMANS, P. and PRESTIANNI, C. 2011. A simple type of wood in two Early Devonian plants. *Science*, **333**, 837.

GRIFFING, D. H., BRIDGE, J. S. and HOTTON, C. L. 2000. Coastal-fluvial palaeoenvironments and plant palaeoecology of the lower Devonian (Emsian), Gaspé Bay, Québec, Canada. *In* FRIEND, P. and BPJ, W. (eds.) *New perspectives on the Old Red Sandstone*, Geological Society Special Publication 180. Geological Society, London, 61–84 pp.

GROOVER, A. T. and SPICER, R. 2010. Evolution of development of vascular cambia and secondary growth. *New Phytologist*, **186**, 577–592.

HOFFMAN, L. A. and TOMESCU, A. M. F. 2013. An early origin of secondary growth: *Franhueberia gerriennei* gen. et sp. nov. from the Lower Devonian of Gaspé (Quebec, Canada). *American Journal of Botany*, **100**, 754–763.

JOY, K. W., WILLIS, A. J. and LACEY, W. S. 1956. A rapid cellulose peel technique in palaeobotany. *Annals of Botany*, **20**, 635–637.

KENRICK, P. and CRANE, P. R. 1997. *The origin and early diversification of land plants*. Smithsonian Institution Press, Washington.

KOTYK, M. E., BASINGER, J. F., GENSEL, P. G. and DE FREITAS, T. A. 2002. Morphologically complex plant macrofossils from the Late Silurian of Arctic Canada. *American Journal of Botany*, **89**, 1004–1013.

MATSUNAGA, K. K. S., STOCKEY, R. A. and TOMESCU, A. M. F. 2013. *Honeggeriella complexa* gen. et sp. nov., a heteromerous lichen from the lower cretaceous of Vancouver Island (British Columbia, Canada). *American Journal of Botany*, **100**, 450–459.

MATTEN, L. C. and BANKS, H. P. 1967. Relationship between the Devonian progymnosperm genera *Sphenoxylon* and *Tetraxylopteris*. *Bulletin of the Torrey Botanical Society*, **94**, 321–333.

MCGREGOR, D. C. 1977. Lower and Middle Devonian spores of eastern Gaspé, Canada II. Biostratigraphy. *Palaeontographica Abt. B*, **163**, 111–142.

PFEILER, K. C. and TOMESCU, A. M. F. 2020. Data from: An Early Devonian actinostelic euphyllophyte with secondary growth from the Emsian of Gaspé (Canada) and the importance of tracheid wall thickening patterns in early euphyllophyte systematics. Dryad Digital Repository. https://doi.org/10.5061/dryad.zgmsbcc7n

R CORE TEAM. 2018. R: A language and environment for statistical computing.

REMY, W. and HASS, H. 1986. *Gothanophyton zimmermanni* nov. gen., nov. spec., eine Pflanze mit komplexem Stelär-Körper aus dem Emsian. *Argumenta Palaeobotanica*, **7**, 9–69.

STRULLU-DERRIEN, C., KENRICK, P., TAFFOREAU, P., COCHARD, H., BONNEMAIN, J. L., LE HÉRISSÉ, A., LARDEUX, H. and BADEL, E. 2014. The earliest wood and its hydraulic properties documented in c. 407-million-year-old fossils using synchrotron microtomography. *Botanical Journal of the Linnean Society*, **175**, 423–437.

TOLEDO, S. 2018. A new anatomically-preserved plant form the Lower Devonian of Quebec (Canada): implications for euphyllophyte phylogeny and early evolution of structural complexity. MSc thesis. Humboldt State University, 1–101pp.

———, BIPPUS, A. C. and TOMESCU, A. M. F. 2018. Buried deep beyond the veil of extinction: euphyllophyte relationships at the base of the spermatophyte clade. *American Journal of Botany*, **105**, 1264–1285.

TOMESCU, A. M. F. and GROOVER, A. T. 2019. Mosaic modularity : an updated perspective and research agenda for the evolution of vascular cambial growth. *New Phytologist*, **222**, 1719–1735.

Figures

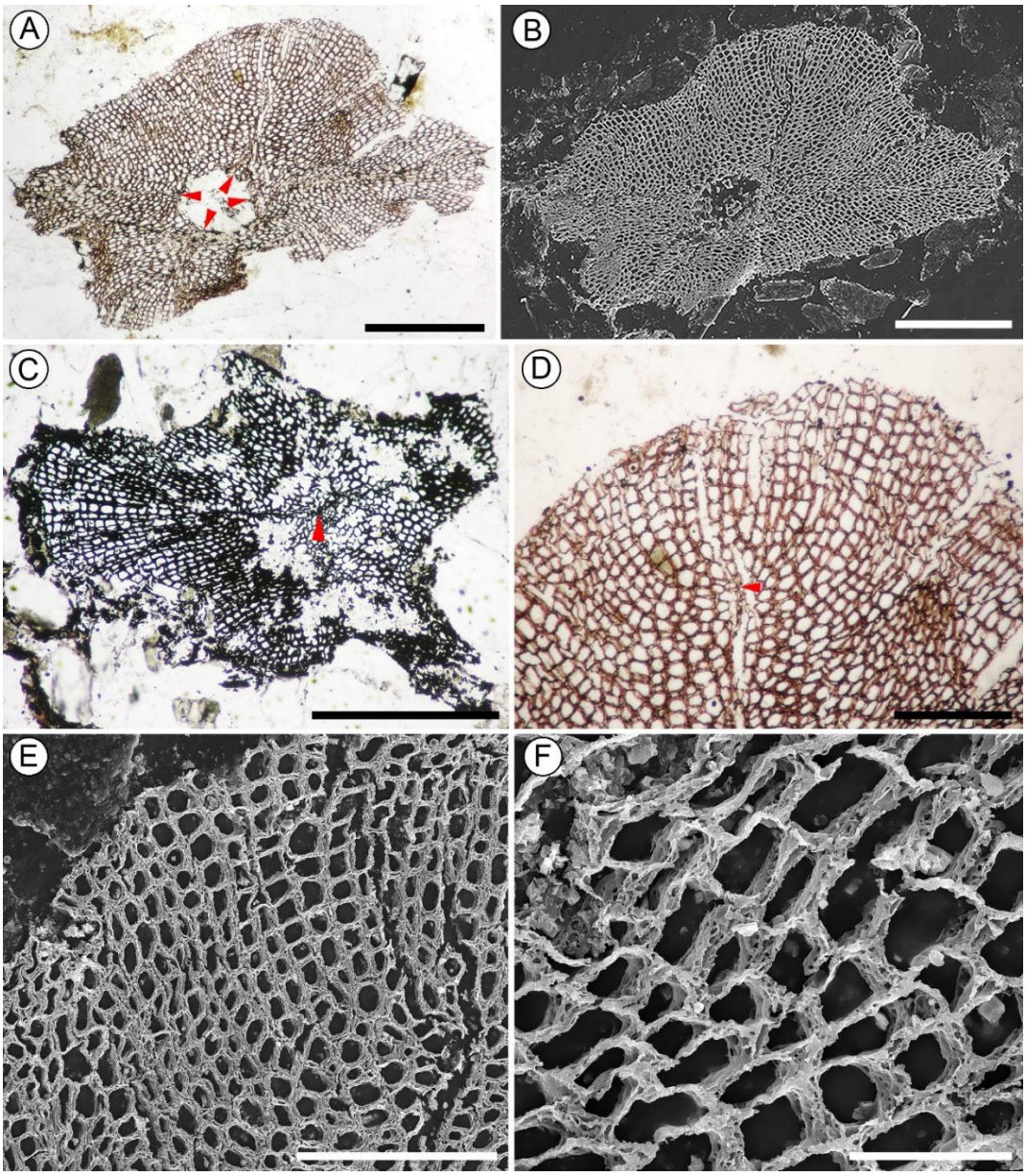

Figure 1. ***Gmujij tetraxylopteroides*** **gen. & sp. nov.** xylem anatomy. A, Axis cross section illustrating four-lobed mesarch primary xylem and secondary xylem; note central area of missing tissue interpreted as putative evidence of detritivory. Arrowheads indicate midplanes of primary xylem lobes wherein protoxylem strands are positioned. USNM 557840 Gbot #84c. Scale bar = 500 µm. B, Scanning electron micrograph of axis cross section comparable to section in A. USNM 557840 Gbot #101c. Scale bar =

500 µm. C, Axis cross section of charcoalified specimen with partial preservation of central primary xylem; arrowhead indicates putative central protoxylem strand. USNM 557840 Itop #16a. Scale bar = 500 µm. D, Cross section of xylem lobe showing transition from metaxylem to secondary xylem; note radially aligned secondary xylem tracheids and metaxylem tracheids with slight radial elongation. Arrowhead indicates position of mesarch protoxylem strand at the tip of the primary xylem lobe. USNM 557840 Gbot #84C. Scale bar = 200 µm. E, Scanning electron micrograph of radially aligned secondary xylem tracheids. USNM 557840 Gbot #101c. Scale bar = 200 µm. F, Scanning electron micrograph; detail of secondary xylem tracheids. USNM 557840 Gbot #101c. Scale bar = 50 µm.

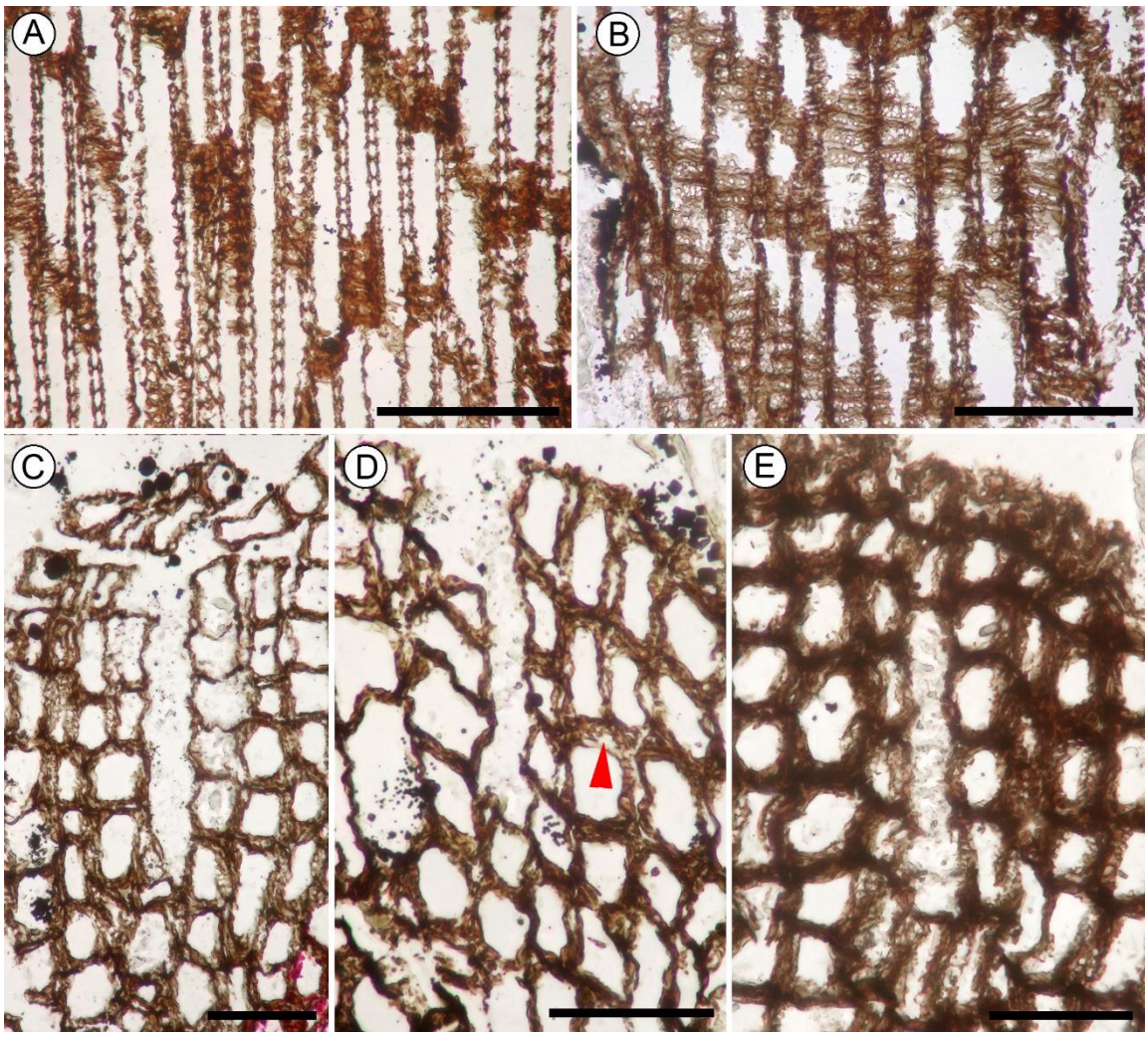

Figure 2. *Gmujij tetraxylopteroides* gen. & sp. nov. tracheid pitting and rays. A, B, Longitudinal sections of metaxylem (A) and secondary xylem (B) consisting of tracheids with *Psilophyton*-type (P-type) thickenings. USNM 557840 G2side #4a. Scale bars = 200 µm. C, Split between two radial files of secondary xylem tracheids due to taphonomic causes. USNM 557840 Gbot #85c. Scale bar = 100 µm. D, E, Rays in the secondary xylem. Note abrupt ending of radial tracheid files at the inner end (bottom) of the rays and the outer end of the ray in E enclosed by tracheids. Arrowhead (D) indicates a multiplicative division. D: USNM 557840 Gbot #84c, scale bar = 100 µm; E: USNM 557840 Gbot #74c, scale bar = 100 µm.

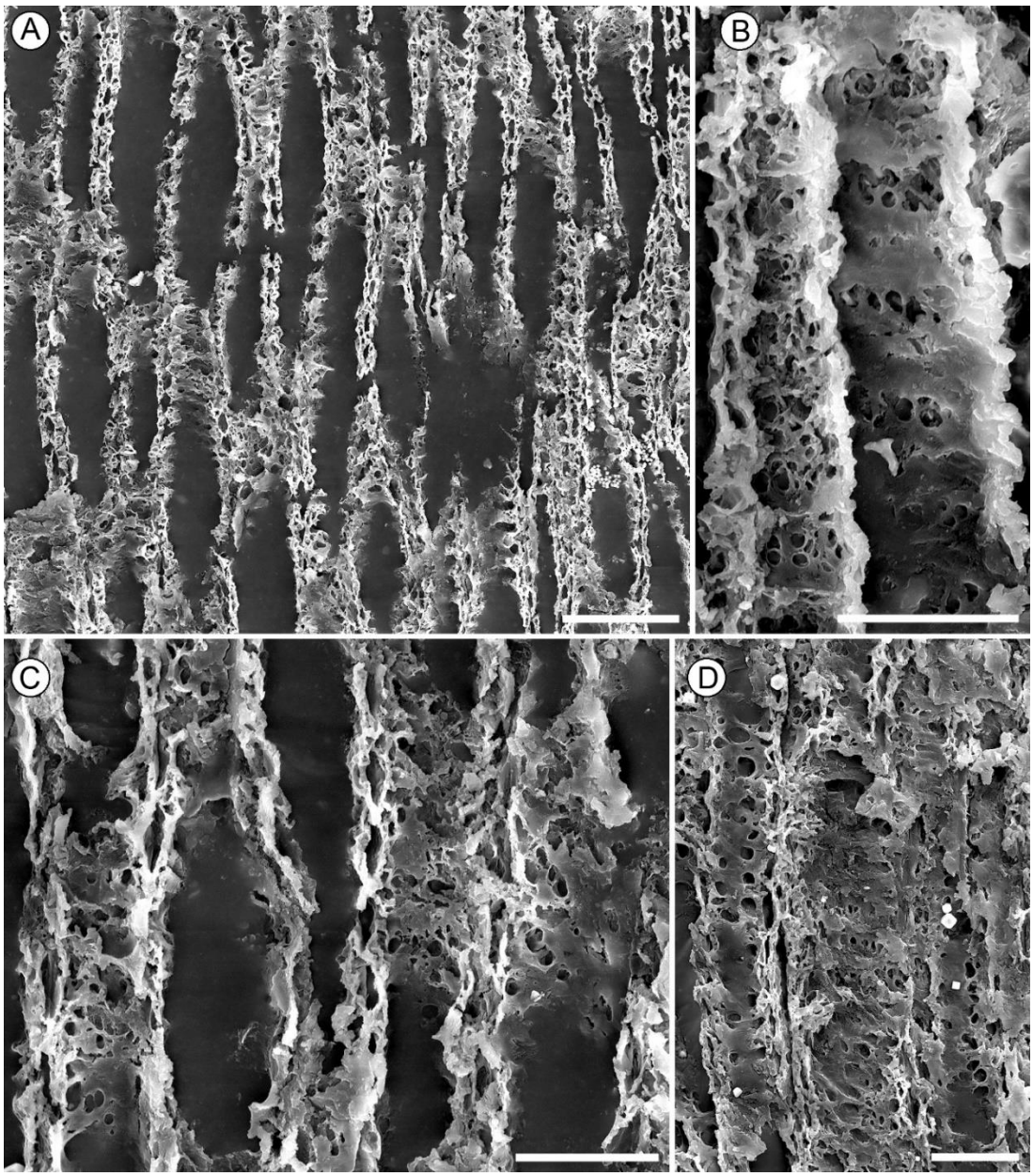

Figure 3. ***Gmujij tetraxylopteroides*** **gen. & sp. nov.** tracheid anatomy (scanning electron micrographs of longitudinal sections). A, Metaxylem tracheids with P-type thickenings in longitudinal transverse section. Scale bar = 50 µm. B, Secondary xylem tracheid with P-type thickenings; note biseriate apertures in some of the pits. Scale bar = 25 µm. C, Detail of metaxylem tracheids showing lenticular pit pair chambers in longitudinal transverse section. Scale bar = 25 µm. D, Detail of metaxylem tracheids; note uniseriate circular bordered pits in narrow tracheid (top left). Scale bar = 25 µm. All images USNM 557840 G2side #3A.

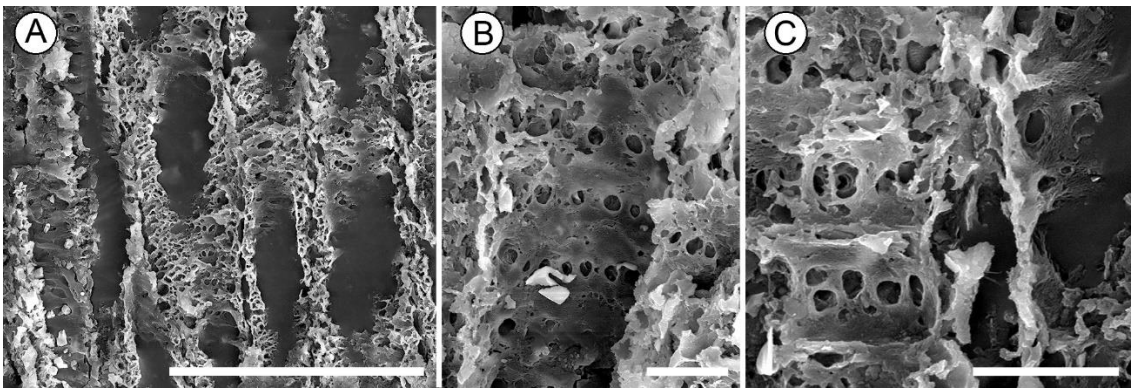

Figure 4. ***Gmujij tetraxylopteroides*** **gen. & sp. nov.** tracheid anatomy (scanning electron micrographs of longitudinal sections). A, Metaxylem tracheids with P-type thickenings in longitudinal transverse section; lenticular pit pair chambers and porous structure of tracheid wall thickenings. Scale bar = 50 µm. B, Secondary xylem tracheids with uniseriate apertures of P-type thickenings. Scale bar = 12.5 µm. C, Detail of apertures in P-type thickenings of secondary xylem tracheids. Scale bar = 12.5 µm. All images USNM-557840 G2side #3a.

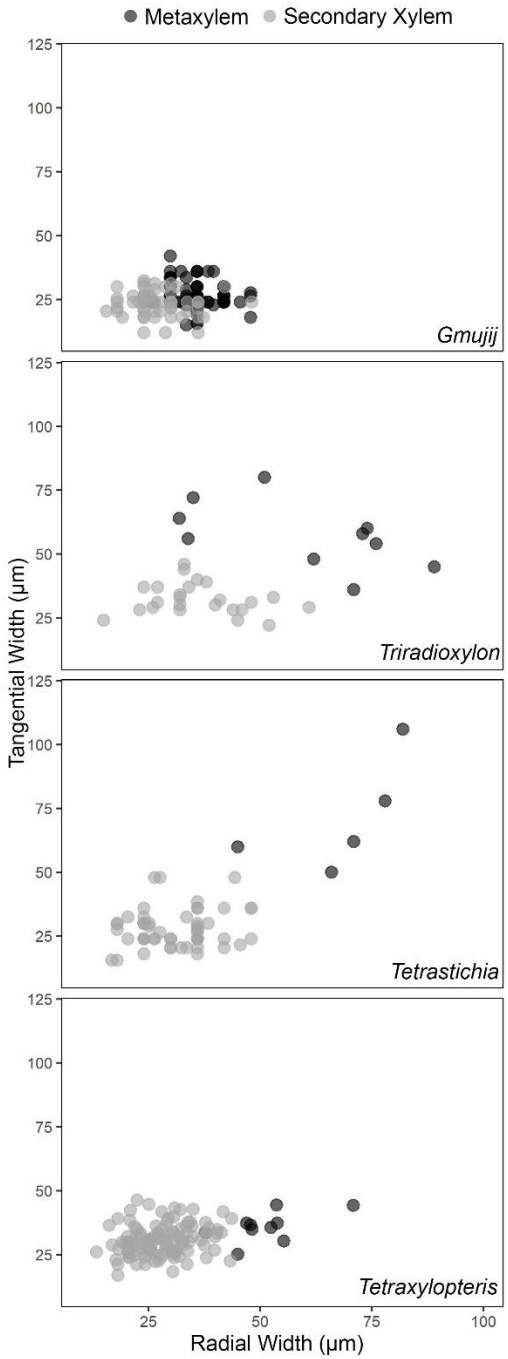

Figure 5. Comparisons of metaxylem (dark gray) and secondary xylem (light gray) tracheid width.

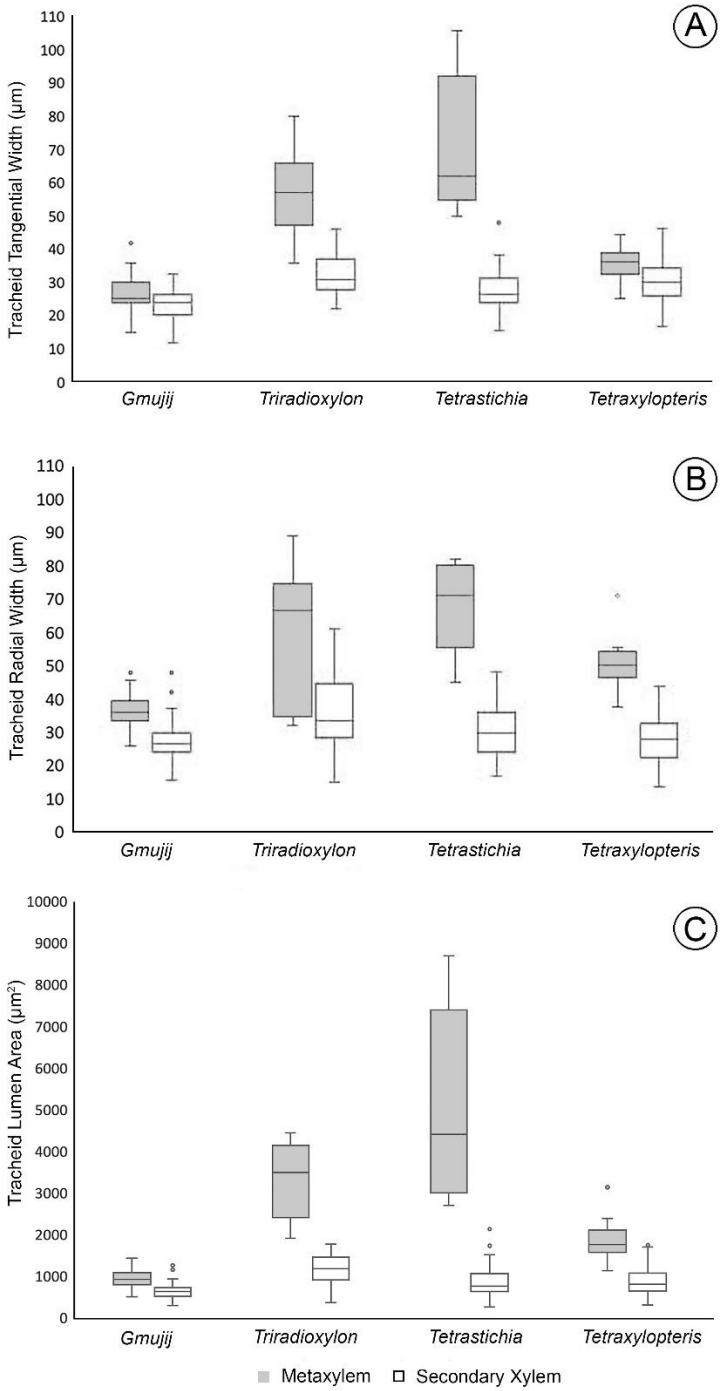

Figure 6. Comparisons of metaxylem (light grey) and secondary xylem (white) tracheid width (A, B) and tracheid cross-sectional lumen area (C). Boxes represent the interquartile ranges with medians as horizontal bars; whiskers represent the first and third quartile. See also summary statistics (Appendix).

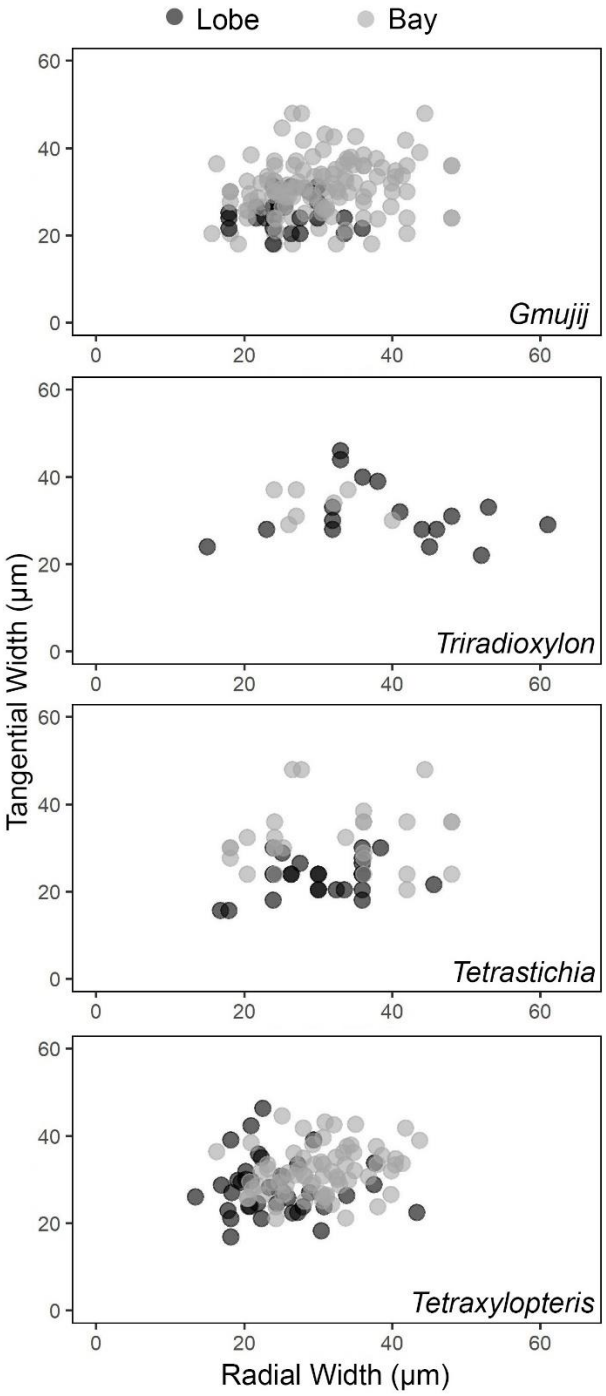

Figure 7. Comparisons of secondary xylem tracheid width, measured in files from the areas around the tips of primary xylem lobes (Lobe files; dark grey) and in files from areas of the embayments between the lobes (Bay files; light grey).

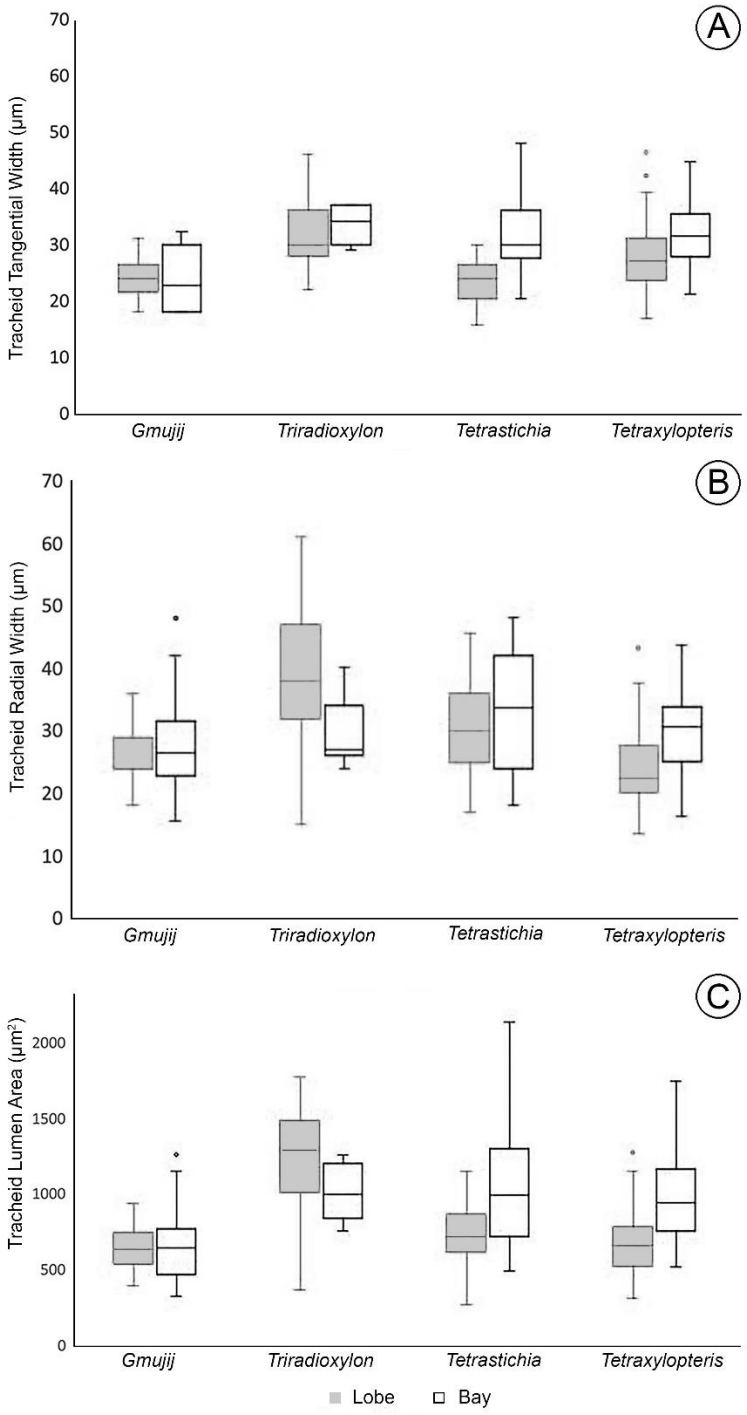

Figure 8. Comparisons of secondary xylem tracheid width (A, B) and tracheid cross-sectional lumen area (C), measured in files from the areas around the tips of primary xylem lobes (Lobe files; gray) and in files from areas of the embayments between the

lobes (Bay files; white). Boxes represent the interquartile ranges with medians as horizontal bars; whiskers represent the first and third quartile. See also summary statistics (Appendix).

.

Appendix

Table 1. Summary statistics for comparisons between metaxylem and secondary xylem tracheid sizes.

Radial tracheid width (µm) of metaxylem.

	Gmujij	*Triradioxylon*	*Tetrastichia*	*Tetraxylopteris*
Min	26.0	32.0	45.0	70.9
Max	48.0	89.0	82.0	37.7
N	72.0	10.0	5.0	10.0
Median	36.0	66.5	71.0	50.3
Mean	36.2	59.7	68.4	51.2

Radial tracheid width (µm) of secondary xylem.

	Gmujij	*Triradioxylon*	*Tetrastichia*	*Tetraxylopteris*
Min	15.6	15.0	16.8	13.4
Max	48.0	61.0	48.0	43.7
N	58.0	24.0	53.0	109.0
Median	26.4	33.5	30.0	28.0
Mean	27.1	36.4	31.2	28.1

Tangential tracheid width (µm) of metaxylem.

	Gmujij	*Triradioxylon*	*Tetrastichia*	*Tetraxylopteris*
Min	15.0	36.0	50.0	25.1
Max	42.0	80.0	106.0	44.4
N	72.0	10.0	5.0	10.0
Median	25.2	57.0	62.0	36.1
Mean	26.5	57.3	71.2	35.9

Tangential tracheid width (µm) of secondary xylem.

	Gmujij	*Triradioxylon*	*Tetrastichia*	*Tetraxylopteris*
Min	12.0	22.0	15.6	16.8
Max	32.4	46.0	48.0	46.3
N	58.0	24.0	53.0	109.0
Median	24.0	31.0	26.4	30.0
Mean	23.5	32.3	27.8	30.6

Cross-sectional surface area of tracheids (tangential x radial width) (µm^2) in metaxylem.

	Gmujij	*Triradioxylon*	*Tetrastichia*	*Tetraxylopteris*
Min	504	1904.0	2700.0	1129.5
Max	1425.6	4440.0	8692.0	3133.78
N	72.0	10.0	5.0	10.0
Median	921.6	3490.5	4402.0	1753.1
Mean	951.8	3286.7	5035.6	1864.49

Cross-sectional surface area of tracheids (tangential x radial width) (µm^2) in secondary xylem.

	Gmujij	*Triradioxylon*	*Tetrastichia*	*Tetraxylopteris*
Min	288.0	360.0	262.1	305.8
Max	1260.0	1769.0	2131.2	1744.4
N	58.0	24.0	53.0	109.0
Median	633.6	1172.0	756.0	808.6
Mean	634.5	1162.3	877.7	869.3

Table 2. Summary statistics for comparisons of sizes of secondary xylem tracheids that are located in either the areas around the tips of primary xylem lobes (lobe) or the areas in the embayments between lobes (bay).

Radial tracheid width (µm) in the areas around the tips of primary xylem lobes (lobe).

	Gmujij	*Triradioxylon*	*Tetrastichia*	*Tetraxylopteris*
Min	18.0	15.0	16.8	13.4
Max	36.0	61.0	45.6	43.3
N	27.0	17.0	26.0	38.0
Median	24.0	38.0	30.0	22.5
Mean	25.7	39.1	30.6	24.3

Radial tracheid width (µm) in the areas in the embayments between lobes (bay).

	Gmujij	*Triradioxylon*	*Tetrastichia*	*Tetraxylopteris*
Min	15.6	24.0	18.0	16.2
Max	48.0	40.0	48.0	43.7
N	18.0	7.0	27.0	71.0
Median	26.4	27.0	33.6	30.5
Mean	27.6	30.0	31.8	30.1

Tangential tracheid width (µm) in the areas around the tips of primary xylem lobes (lobe).

	Gmujij	*Triradioxylon*	*Tetrastichia*	*Tetraxylopteris*
Min	18.0	22.0	15.6	46.3
Max	31.2	46.0	30.0	39.1
N	27.0	17.0	26.0	38.0
Median	24.0	30.0	24.0	27.1
Mean	24.9	31.7	23.3	28.3

Tangential tracheid width (µm) in the areas in the embayments between lobes (bay).

	Gmujij	*Triradioxylon*	*Tetrastichia*	*Tetraxylopteris*
Min	18.0	29.0	20.4	21.1
Max	32.4	37.0	48.0	44.6
N	18.0	7.0	27.0	71.0
Median	22.8	34.0	30.0	31.9
Mean	23.7	33.6	32.2	31.1

Cross-sectional surface area of tracheids (tangential x radial width) (µm^2) in the areas around the tips of primary xylem lobes (lobe).

	Gmujij	*Triradioxylon*	*Tetrastichia*	*Tetraxylopteris*
Min	388.8	360.0	262.1	305.8
Max	936.0	1769.0	1152.0	1270.9
N	27.0	17.0	26.0	38.0
Median	633.6	1288.0	720.0	653.7
Mean	639.3	1227.6	719.8	684.6

Cross-sectional surface area of tracheids (tangential x radial width) (µm^2) in the areas in the embayments between lobes (bay).

	Gmujij	*Triradioxylon*	*Tetrastichia*	*Tetraxylopteris*
Min	318.2	754.0	489.6	512.7
Max	1260.0	1258.0	2131.2	1744.4
N	18.0	7.0	27.0	71.0
Median	640.8	999.0	993.6	941.4
Mean	657.1	1003.4	1029.9	968.2

CHAPTER 2: MOSAIC ASSEMBLY OF REGULATORY PROGRAMS FOR VASCULAR CAMBIAL GROWTH: A VIEW FROM THE EARLY DEVONIAN

Introduction

Several recent Early Devonian plant descriptions have uncovered previously unrecognized breadth of anatomical diversity present among early euphyllophytes (Gerrienne *et al.* 2011; Hoffman & Tomescu 2013; Strullu-Derrien *et al.* 2014; Gensel 2018; Toledo 2018; Bickner & Tomescu 2019; Pfeiler & Tomescu in review). These new plants inform our hypotheses of phylogenetic relationships of basal vascular plants and also reveal an unexpected level of diversity and complexity (Toledo *et al.* 2018; Niklas & Crepet 2020) in the early stages of the first major tracheophyte radiation. A prime example of a character that contributes to structural diversity and complexity is the presence of secondary growth, or growth by a lateral cambium (vascular cambium) that results in radially aligned tracheids. Secondary growth originated in the Early Devonian (Armoricaphyton; Gerrienne *et al.* 2011; Strullu-Derrien *et al.* 2014), and rapidly diversified (Hoffman & Tomescu 2013; Gensel 2018; Pfeiler & Tomescu, in review). By the Middle Devonian secondary growth was present in all major euphyllophyte lineages (Cichan & Taylor 1990).

The regulation of secondary growth from a vascular cambium is considered to be a modular assembly (Tomescu & Groover 2019) in which the different developmental processes that, in combination, lead to production of secondary tissues are controlled by

more-or-less independent sets of genetic interactions (regulatory modules). The activity of some of these modules can be recognized in extant, as well as extinct plants based on key structural fingerprints, such as radially aligned tracheids, presence of rays and multiplicative (anticlinal) divisions. Evidence for the modular nature of secondary growth regulation and for the independent deployment of regulatory modules can be traced back to structural features present in euphyllophytes of the Early Devonian.

Here, I describe a new Early Devonian plant, *Perplexa praestigians* gen et sp. nov., that possesses a unique set of characters, including a mesarch protostele and secondary growth, both with features not known in coeval plants. *Perplexa* adds yet another type to the growing list of modes of secondary growth documented in Early Devonian plants – previously including *Franheuberia*, *Armoricaphyton*, and G*mujij* (Gerrienne *et al.* 2011; Hoffman & Tomescu 2013; Pfeiler & Tomescu, in review), as well as several other, as yet unnamed, plants (Gerrienne *et al*. 2011; Toledo *et al*. 2017; Gensel 2018). These plants that are early representatives of the euphyllophyte clade and mark the earliest occurrences of secondary growth, exhibit a spectrum of combinations of structural fingerprints that illustrate different patterns of expression of regulatory modules acting in secondary growth. The anatomy of secondary xylem in these plants reinforces existing hypotheses about the modular regulation of vascular cambial growth and illustrates different degrees of canalization and mosaic expression of regulatory modules in coeval early tracheophytes.

Materials and Methods

The plant material is preserved by cellular permineralization with calcium carbonate in a cobble collected in 1965 by Dr. Francis M. Hueber (Smithsonian Institution – U.S. National Museum of Natural History) from an exposure of the Battery Point Formation on the south shore of Gaspé Bay, near Douglastown (Quebec, Canada). The allochthonous assemblages that host this and other permineralized fossil plants are late Emsian in age, ca. 402-394 Ma old (Hoffman & Tomescu 2013), and hosted by sediments deposited in braided-fluvial to coastal environments (Cant & Walker 1976; Griffing *et al.* 2000).

Serial anatomical sections were obtained using the cellulose acetate peel technique (Joy *et al.* 1956). Peels were mounted with Eukitt (O. Kindler, Freiburg, Germany) for bright field microscopy. Images were captured using a Nikon Coolpix 8800VR digital camera mounted on a Nikon E400 compound microscope and an Olympus Dp73 digital camera mounted on an Olympus SZX16 microscope. Scanning electron micrographs were generated using a FEI Quanta 250 (Hillsboro, Oregon, USA) from cellulose acetate peels prepared using the method detailed in Matsunaga *et al*. (2013). Images were processed using Adobe Photoshop (San Jose, California, USA). Tracheid size measurements were performed in ImageJ (US National Institutes of Health; https://imagej.nih.gov/ij) using slides of fossil material for *Perplexa*.

Measurements for tracheid comparisons were performed on figures 8, 9, 19, and 68 of Banks *et al.* (1975) for *Psilophyton dawsonii*; figure 6.9 of Beck (1979, 1981) for

Archaeopteris (*Callixylon*) sp.; and figures 20, 21, 61, and 81 of Dennis (1974) for *Zygopteris illinoiensis* and *Z. berryvillensis*. In the metaxylem I measured the largest well-preserved tracheids for size comparisons. For roundness and circularity, published images of *Zygopteris*, *Psilophyton*, and *Archaeopteris* were enhanced using Photoshop for contrast and resolution, and measurements were obtained using ImageJ. In these measurements, circularity is calculated as 4π*area/perimeter^2 (a value of 1.0 indicates a perfect circle; as the value approaches 0.0, it indicates an increasingly elongated shape); roundness, a measure of angularity (Szerakowska *et al.* 2015), is calculated as 4*area/(π*major_axis^2), or the inverse of the aspect ratio. Double boxplots of circularity and roundness were produced in R using the package boxplotdbl (Tomizono 2013; R Core Team 2018). In the secondary xylem I selected well-preserved radial tracheid files within which all tracheids were measured for radial and tangential width. In each file I measured only the first 10 tracheids to ensure that I was comparing equivalent developmental stages among the four plants. Summary statistics of measurements and box plots were obtained using Microsoft Excel. When making comparisons between plants (in the Results and Discussion sections) I refer to average tracheid widths, unless otherwise noted. All measurement data used in comparisons are deposited as supplemental data hosted on the Theses and Projects web page (Digital Commons, Humboldt State University, Arcata, California; https://digitalcommons.humboldt.edu/etd/). Cobble slabs, acetate peels, slides, and SEM stubs are stored at the Smithsonian Institution – U.S. National Museum of Natural History under collection number USNM 557820-4.

Results

Systematics

Division: Tracheophyta Cavalier-Smith 1998

Subdivision: Euphyllophytina Kenrick & Crane 1997

Perplexa Pfeiler et Tomescu gen. nov.

Generic diagnosis: Axes with central protostelic primary xylem, with or without surrounding layer of secondary xylem. Primary xylem mesarch with variable number of protoxylem poles distributed equidistantly close to the periphery of the metaxylem and decreasing distally. Metaxylem tracheids with scalariform thickenings, bordered pits and *Psilophyton*-type thickenings. Secondary xylem with multiplicative divisions and a radial component consisting of radially expanded tracheids and radially-curved tracheid ends. Secondary xylem tracheids with *Psilophyton*-type thickenings. Inner cortex parenchymatous; outer cortex robust, sclerenchymatous, with gaps representing substomatal chambers.

Etymology: *Perplexa*, in reference to the perplexing combination of xylem characters that preclude taxonomic placement

Perplexa praestigians Pfeiler et Tomescu sp. nov.

Specific diagnosis: Axis diameter varies from 2.6-3.3 mm. Epidermis of small cells with thickened walls; sclerified outer cortex up to seven cells wide, 0.45-0.29 mm thick. Outer cortical cells prismatic, up to 480 µm tall and 72 x 132 µm in cross sections and with thick (12-27 µm) secondary walls. Inner cortical cells parenchymatous, 60-153 µm tall, 46.5-63 µm wide. Substomatal chambers in outer cortex. Primary xylem 0.8 mm in diameter. Metaxylem tracheids with bordered pits 12 µm in diameter; pit apertures circular 2-4 µm in diameter. Metaxylem tracheids ~ 31.1 µm in diameter, cell walls 3.6 µm in width and *Psilophyton*-type thickenings with horizontal bars ~ 3.6 µm in height, distance between the bars 3-6 µm, and multiple pit apertures up to 3 µm in diameter. Secondary xylem tracheids with irregular sizes (c. 50.5 µm in radial width, 29.1 µm in tangential width) and shapes, and walls conspicuously thicker than those of metaxylem tracheids; some tracheids with radial orientation and some tracheids with ends curved and expanding in radial direction. Secondary xylem tracheids with *Psilophyton*-type pitting; height of the scalariform bars up to 5.7 µm and distance between bars ~ 4.5 µm. Membranes between horizontal bars with uni- or multiseriated apertures ~3.5 µm in diameter. Multiplicative divisions infrequent.

Etymology: *praestigians* for Latin *praestigiator* (deceiver), in reference to the misleading similarity of the primary xylem, when taphonomically distorted (crushed), to that of *Psilophyton*.

Holotype: Axis in specimen 557820-4, slabs B, C, D.

Locality and horizon: South shore of Gaspé Bay, in the vicinity of Douglastown, Quebec, Canada; Battery Point Formation, mid- to late Emsian (Early Devonian), ca. 402–394 million years.

Description

Perplexa praestigians is represented by one unbranched axis fragment. The axis consists of a central strand of protostelic primary xylem surrounded by a layer of xylem with radially aligned tracheids interpreted as secondary xylem (present only in the basal portion of the axis), a zone lacking complete cellular preservation and interpreted as an inner cortex layer, and a sclerified outer cortex (Figure 1). The fragment is at least 3 cm in total length (one of its ends is still embedded in the rock matrix and has not been exposed by sectioning) (Figure 3B). The diameter of the axis varies along the fragment and the epidermis is partially preserved (Figures 3A, 3B). In basal portions of the axis, where secondary growth is present, the overall diameter of the plant is 2.64 mm (Figures 1B, 1C, 3B). Interestingly, the diameter of the plant is larger, 3.3 mm, in the most distal region of the axis, where secondary growth is not present (Figure 1). In contrast to this pattern, the overall diameter of the xylem varies between 1.53 mm in basal portions of the axis and 0.83 mm in its distal region (Figures 2A, 2C, 2E, 2G, 3A, 3B).

Epidermis and sclerified cortex. An incompletely preserved epidermis is present in some regions of the axis. Where preserved, the cells are smaller than the adjacent

cortical cells, round or rectangular in shape, and bounded by a thin, dark organic layer, which may represent the cuticle (Figure 4). In other places, epidermal cells are conspicuously abraded partially, so that only their inner periclinal walls and portions of the anticlinal walls protrude from the axis surface (Figure 4C). In yet other instances, a light-colored amorphous layer, bounded by the thin organic layer interpreted as cuticle, covers the axis surface. The positional correlation of this layer with portions of preserved epidermis (Figure 4A) suggests that it represents a gap left by the incompletely preserved epidermis.

The sclerified outer cortex, up to seven cells wide, is 0.45 mm thick at the base of the axis and 0.29 mm thick in the distal portion (Figure 3A). Better preserved in the basal region of the axis, the outer cortex consists of prismatic cells with rectangular cross section, 42-132 µm in radial width and 30-72 µm in tangential width (Figures 3A, 4). In longitudinal section, the cells are up to 480 µm in length (Figure 5A, 5B, 5D). The robust secondary walls of these cells are 12-27 µm thick. The outer cortical layer as seen in cross sections exhibits numerous discontinuities (Figures 1A, 1B, 3A, 4B). While some of these may have taphonomic causes, longitudinal sections indicate that many of the discontinuities correspond to gaps in the outer cortex that have consistent size and orientation, and a relatively regular arrangement (Figure 5B, 5C). The gaps are up to 180 µm wide and are vertically elongated, 550 µm tall. Their regular size and arrangement indicate that they correspond to substomatal chambers, of the type seen in other Early Devonian plants with similar cortical organization, such as *Psilophyton* (Banks *et al.* 1975) and *Tainioxyla* (Bickner & Tomescu 2019). Direct evidence for stomata is

difficult to obtain, due to the incomplete preservation of the epidermis. The transition between the sclerenchymatous outer cortex and the parenchymatous inner cortex is sharp. When preserved, especially in areas adjacent to the outer cortex, inner cortical cells are slightly elongated vertically, 60-153 µm tall and 46.5-63 µm wide (Figure 5A, 5B).

Primary xylem. The central primary xylem strand consists of a mesarch protostele (Figure 2). The primary xylem is roughly 0.8 mm in diameter the entire length of the axis. Protoxylem strands are located close to the periphery and consist of tracheids ca. 12 µm in diameter with annular thickenings 2-3.5 µm in width (Figure 8A, 8B). The number of protoxylem poles varies along the axis (Figures 2, 3D). In the proximal portion of the axis fragment there are 10 protoxylem poles distributed fairly equidistantly close to the periphery of the metaxylem, giving it a slightly stellate outline (Figures 2G, 3D). The number of protoxylem poles decreases distally. For example, within a 250-300 µm distance in the basal portion of the axis, the number of protoxylem poles decreases from 10 to six (Figures 2F, 2H, 3D). The decrease in the number of protoxylem poles along the axis is paralleled by a centripetal shift of the remaining poles, which form two groups with diametrically opposite location (Figures 2B, 2D, 2F, 3D). In the most distal portion, only two protoxylem poles seem to be present. However, the central region of the xylem is slightly compressed in the distal portion, rendering observation of the distinct protoxylem poles difficult. Importantly, the distal portion of the axis looks strikingly similar in anatomy to *Psilophyton* (Banks *et al.* 1975; Trant & Gensel 1985).

Secondary xylem. Tracheids of the secondary xylem have conspicuously thicker cell walls (10 μm) and larger overall size than those of the metaxylem (Table 1). The secondary xylem reaches its maximum thickness of 0.6 mm - up to 10 tracheids per file - in the most basal sections (Figure 3B, 3C). Tracheids at the periphery of the secondary xylem have smaller radial diameters and thinner cell walls that are sometimes missing the outer periclinal portion. Interestingly, tracheids in penultimate position within radial files, are also smaller in diameter but possess fully developed, thick secondary walls (Figure 2G). The number of cells per radial file decreases acropetally and the layer of radially aligned tracheids is lacking from the distal portion of the axis fragment (Figure 3B, 3C). Typical parenchymatous rays, as seen in other Early Devonian plants with secondary growth (*Armoricaphyton*, *Franhueberia*), are absent. Multiplicative divisions are present but infrequent (Figure 6).

Despite the conspicuous radial alignment of tracheids in this layer, their patterning exhibits striking departures from the typical regular patterning of tissues produced by a cambial layer with fully coordinated activity. (1) The tracheids have irregular sizes and shapes, as seen in cross sections: most are rectangular, whereas others have triangular or polygonal shapes; there are wide differences in tangential or radial size even between adjacent tracheids. (2) Adjacent radial files of tracheids may exhibit strikingly different numbers of tracheids, whose periclinal walls are offset radially (Figure 2G). (3) Cross sections of the axis also exhibit relatively frequent instances of tracheids with radial orientation (Figure 7A, 7B, 7C); longitudinal radial (Figure 7D, 7E) and tangential sections (Figure 7G, 7H) through the secondary xylem demonstrate that in

the majority of cases these represent the ends of regularly oriented tracheids that curve sharply in a radial direction. (4) In longitudinal radial sections, some tracheids are very short and wide (twice as wide as those vertically adjacent) (Figure 7F); such instances probably correspond to the narrow, radially elongated tracheids observed in cross sections (Figure 2G). (5) A rare instance of a radially elongated cell devoid of secondary wall thickenings surrounded by tracheids at the transition between metaxylem and secondary xylem (Figure 7I) indicates that parenchyma could differentiate within the xylem.

Tracheid anatomy and thickening patterns. The tracheid thickening patterns vary laterally from protoxylem to the secondary xylem (Figure 8). Some metaxylem cells show typical scalariform thickenings (Figure 8C). The P-type thickening pattern of the majority of metaxylem tracheids exhibits a broad range of variability in terms of the shape, size, and number of apertures present between the horizontal bars of this thickening type. In very narrow metaxylem tracheids directly adjacent to the protoxylem tracheids and ca. 12 µm in diameter, single bordered pits are present between the bars (Figure 8A, 8D); the pit apertures are circular and measure 2-4 µm in diameter. In wider tracheids positioned farther from the protoxylem, as well as in the tapered ends of otherwise wider tracheids, the membrane between the bars may exhibit 2-3 small apertures (Figure 8B, 8E) or one large, oval and horizontally elongated aperture (Figure 8A, 8B, 8C, 8E). Metaxylem cells that are not directly adjacent to protoxylem are angular to circular in cross section, measure average 31.1 µm in diameter (9.0-60.0 µm; n

= 91), have cell walls 3.6 µm in width and have tapered ends. These cells have P-type thickenings with horizontal bars up to 3.6 µm in height, distance between the bars is 3-6 µm, and the pit apertures up to 3 µm in diameter.

Secondary xylem tracheids are also characterized by P-type pitting. They are radially elongated, average 50.5 µm in radial width (23.0-72.0 µm; n = 46) and 29.1 µm in tangential width (11.0-42.0 µm; n = 56). The height of the scalariform bars that form the P-type thickening of the secondary xylem is up to 5.7 µm in height and the distance between these bars is up to 4.5 µm. The membranes between the horizontal bars feature uni- or multiseriated files of apertures up to 3.5 µm in diameter (Figure 7D, 7E).

In addition to the features of P-type thickenings described above, *Perplexa praestigians* shows a broad range of variation in the geometry of the elements that form the structure of this thickening pattern, when compared to the description of *Psilophyton dawsonii* by Hartman & Banks 1980 (also illustrated by Kenrick & Crane 1997). The width of the combined pit chambers in a pit pair (as seen in longitudinal sections; Figure 8B) is much narrower than in *P. dawsonii*. The bars of secondary wall material that form the general scalariform pattern of the thickenings may protrude more or less into the lumen of tracheids (compare Figure 8B and Figure 8D). In thickenings with strongly protruding bars, the pit membrane that bears the aperture(s) is located at a level closer to the primary wall than to the “crests” of the bars (Figures 8D, 9D). Finally, the bars of secondary wall material are denser – with a spongy structure (Figure 9) – than those of *P. dawsonii*, which are hollow.

Comparisons

Tracheid sizes. *Perplexa* is similar in its mesarch xylem maturation and possession of secondary xylem to multiple younger plants. Of these, based on close anatomical similarity, I compare it to small, protostelic stems of *Archaeopteris*/*Callixylon* (Devonian; Beck 1979, 1981) and to *Zygopteris* (Pennsylvanian; Dennis 1974); although described as exarch by Dennis (1974), the primary xylem of *Zygopteris illinoiensis* is mesarch upon close examination. Both these younger plants have metaxylem tracheids that are >20 µm wider than those of *Perplexa* (Figure 10A; Table 1). The secondary xylem tracheids of *Archaeopteris* have radial widths that are 17 µm smaller than those of *Perplexa* (Figure 10B; Table 2); however, radial tracheid widths in the secondary xylem are similar in these two plants. *Zygopteris*, on the other hand, has secondary xylem tracheids significantly larger than those of *Perplexa* in both radial and tangential dimensions.

In the distal portion of the axis of *Perplexa*, the metaxylem in the central area is compressed (Figure 2A-F), which gives it the appearance of centrarch xylem maturation. As a result, the distal part of the axis looks very similar anatomically to the coeval plant *Psilophyton dawsonii*, described initially by Banks *et al.* (1975), which has centrarch primary xylem maturation. Comparison of the two plants shows that they have similar sized metaxylem tracheids (Figure 10A; Table 1). Banks *et al.* (1975) also describe axes with radially aligned tracheids that occur in the proximity of a *P. dawsonii* main axis, and they assign these axes to *P. dawsonii*. This led us to compare these radially aligned tracheids to those in the secondary xylem of *Perplexa*.

A brief parenthesis is necessary here to consider the assignment of the axes with radially aligned tracheids to *P. dawsonii* by Banks *et al*. (1975). This assignment is untenable for several reasons: (1) Banks *et al*. do not provide direct evidence for physical connection between the axes bearing radially aligned tracheids and those possessing primary xylem anatomy typical of *Psilophyton*; (2) xylem anatomy of the axes with radially aligned tracheids, in central areas where they lack radial alignment is unlike that of *P. dawsonii* (and in some cases these axes lack non-radially aligned tracheids entirely); (3) if the radially aligned tracheids represent secondary xylem, it is unlikely that such tissues would be produced on a subordinate lateral branch of a main axis that lacks them.

Irrespective of whether the axes with radially aligned tracheids described by Banks *et al*. belong to *P. dawsonii*, I compare their tracheids to those in the secondary xylem of *Perplexa*. The comparison shows that despite major differences in the organization of the primary xylem, like in the case of the metaxylem tracheids, the radially aligned tracheids of the two plants have similar dimensions, both radially and tangentially (Figure 10B; Table 2), and that in both plants the tangential tracheid widths are smaller than the radial widths.

Metaxylem tracheid roundness and circularity. Comparisons of metaxylem tracheid circularity (a measure of elongation) and roundness (a measure of angularity) discussed here take into account only the interquartile ranges obtained for each genus (Figure 11). Overall, the four plants have relatively high tracheid circularity and roundness, grouping together in the upper right quadrant (>0.5 roundness and >0.5

circularity). Additionally, when considering all four taxa together, circularity has a wider range (medians between 0.6-0.8) than roundness (medians between 0.6-0.7). In other words, tracheids show more variation in elongation than in angularity. Furthermore, all four genera exhibit extensive overlap in roundness values. In terms of tracheid circularity, *Archaeopteris* sets the lowest limit (with tracheids that are the least circular) and *Zygopteris* the highest limit (tracheids that are the most circular). Circularity of tracheids in *Psilophyton* falls between, and overlaps with, the ranges of *Archaeopteris* and *Zygopteris*. The circularity range of *Perplexa* overlaps almost entirely with, and is broader than that of, *Zygopteris*. Perplexa also overlaps partially, in terms of circularity, with *Psilophyton*, but does not overlap at all with *Archaeopteris*.

Discussion

The primary body of *Perplexa*

The primary xylem of *Perplexa* is slightly lobed in cross section, with the lobes protruding outwards into the secondary xylem layer at places and protoxylem strands positioned in these lobes. This is similar to configurations typically produced in the primary xylem by the divergence of traces to lateral appendages. Intriguingly, in *Perplexa*, the lobes of primary xylem and their protoxylem strands do not continue outwards through the secondary xylem and cortex, and no lateral appendages are attached to the axis. Furthermore, the significant change in the number of protoxylem strands along the proximo-distal axis, as well as the positioning of these strands, are also intriguing. A possible explanation for the distal decrease in the number of protoxylem

strands is that the specimen preserves an apoxogenetic stage of development (Eggert 1961). Consistent with an apoxogenetic pattern, the thickness of the secondary xylem layer also decreases distally until completely absent in the top half of the axis segment. Nevertheless, it is clear that additional specimens will be needed to fully understand the significance of these intriguing features for the structure and growth of *Perplexa*. Irrespective of this, the transition from exclusively primary tissues, in the distal portion, to primary and secondary tissues in the basal portion of the *Perplexa* axis may indicate that the 3 cm-long specimen records an interval in the life of the plant long enough to encompass periods that both precede and succeed the onset of cambial activity.

Taxonomy

Like other recently discovered Early Devonian plants of the Battery Point Formation (Bickner & Tomescu 2019, Pfeiler & Tomescu, in review), *Perplexa* exhibits a combination of characters that precludes its placement in any of the well-circumscribed groups of Devonian plants. Its mesarch primary xylem places it among the euphyllophytes, but its plesiomorphic *Psilophyton*-type tracheids exclude it from anatomically similar younger groups that are characterized by mesarch primary xylem. Conversely, despite similarities with *Psilophyton*, the specific type of mesarch architecture of *Perplexa*, characterized by shallow-lobed primary xylem and protoxylem strands very close to the periphery of the latter, is unlike anything seen in coeval plants. Additionally, taxonomic placement of *Perplexa* is also hindered by (1) the lack of

information on appendages and branching pattern, anatomy of trace divergence, etc.; and (2) absence of reproductive structures.

Difficulties in the taxonomic placement of *Perplexa* led us to testing the utility of comparisons with other plants in terms of metaxylem tracheid attributes, as a means of taxonomic differentiation. I focused on circularity and roundness (as seen in axis cross sections), both of which are measures of cell shape. While the comparisons reveal some differences, especially in circularity, they are inconclusive from a taxonomic standpoint. Nevertheless, this type of comparative morphometric approach could be used and expanded upon in studies involving additional taxa and larger sample sizes that may result in more conclusive comparisons. More generally, because comparisons of Early Devonian plants are rendered difficult by a paucity of characters due to their relatively simple anatomy and morphology, a renewed focus on exploring differences at finer scales – as attempted here – is required. Exploring new ways to quantify and compare anatomical details in these Early Devonian plants is crucial to accurately characterizing the diversity of Early Devonian floras.

Most concerning is the fact that in distal regions *Perplexa* looks superficially centrarch and strikingly similar to *Psilophyton*. Without the presence of the more basal parts of the axis, which reveal a large mass of central metaxylem with large tracheids and mesarch xylem maturation, this plant could easily be misidentified as *Psilophyton*. Additionally, my comparisons have shown that *Perplexa* is very similar to *Psilophyton* in the size of metaxylem tracheids. Given that many of the plant axes occurring in the same rock sample as *Perplexa* (and throughout the Gaspé permineralized plant assemblages)

have anatomy that, at first glance, looks like *Psilophyton*, these assemblages may be hosting numerous mis-identified axes. This situation adds to the growing realization that fossils assigned to the genus *Psilophyton* may in fact represent multiple distinct taxa, which, in turn, begs for re-evaluation of *Psilophyton* (Gensel 2018).

Secondary xylem recognition

Historically, some authors have used caution in referring to radially aligned tracheids as a result of cambial growth, especially in the case of very early occurrences of this anatomical feature, or in extinct lineages that lack close living relatives (Dennis 1974, Banks *et al*. 1975, Gensel 2018). Recent fossil discoveries and conceptual advances suggest that such caution is not warranted. First, tissues produced by vascular cambial growth, especially secondary xylem, typically exhibit a set of anatomical features that can be used as criteria for recognition of secondary growth (reviewed by Hoffman & Tomescu 2013). These criteria have been used successfully to demonstrate the presence of secondary xylem in early euphyllophytes of the Early Devonian (Gerrienne *et al*. 2011; Hoffman & Tomescu 2013; Pfeiler & Tomescu in review). Second, the recognition that vascular cambial growth is regulated by a set of interacting but independent regulatory modules has led to the idea that these modules, in different combinations, can produce secondary tissues that represent different modes of secondary growth (Tomescu & Groover 2019). As a result, these different modes of secondary growth may not show all the traditional defining features of tissues produced by vascular cambial growth. Third, a series of recently discovered Early Devonian euphyllophytes with radially aligned

tracheids (Gerrienne *et al*. 2011; Hoffman & Tomescu 2013; Gensel 2018; Pfeiler & Tomescu in review) demonstrate that this feature was more frequent than previously thought early in the evolution of the clade. These fossils illustrate combinations of anatomical features that lend support to the modular view of vascular cambial growth regulation. Together, these considerations indicate that vascular cambial growth had evolved by Early Devonian time and suggest that most of the early euphyllophytes exhibiting radially aligned tracheids do possess secondary tissues produced in different modes of growth. *Perplexa praestigians*, described here, represents one such instance of early secondary growth. *Perplexa* and several coeval euphyllophytes, considered together, demonstrate a mosaic pattern of regulatory module deployment in vascular cambial growth among Early Devonian euphyllophytes.

The mode of secondary growth of *Perplexa praestigians*

The xylem of *Perplexa* consists of a central core of tracheids with no specific patterning (other than that produced by the positioning of protoxylem strands and xylem maturation) surrounded by a layer of xylem in which tracheids exhibit conspicuous radial arrangement. This layer possesses a series of characters that are consistent with vascular cambial growth. First, the layer of radially aligned tracheids is conspicuously different from the central xylem in terms of tracheid size, geometry, and wall thickness, which indicates that this layer was formed under different developmental regulation than the central core of xylem. Second, the thickness of this layer decreases acropetally and the layer is absent in the distal parts of the axis (Figure 3B, C). Such a pattern characterizes

the transition from primary growth to secondary growth in extant plants undergoing vascular cambial growth and also documented in the coeval *Armoricaphyton* (Gerrienne & Gensel 2016). Third, most of the cells present around the periphery of the xylem are thinner-walled and sometimes have incompletely preserved periclinal walls (Figures 1C, 4B, 4C, 6). This pattern is consistent with centrifugal addition of new cells – which are less mature, with thinner and incompletely lignified walls, and lower preservation potential – by a lateral meristem. Fourth, multiplicative divisions are present, indicative of anticlinal divisions in the initials of a lateral meristem (Figure 6). Lastly, a radial component is present in the layer of radially aligned tracheids. While this radial component does not consist of typical parenchymatous rays, it includes tracheids that exhibit preferential radial orientation (i.e., regular longitudinally oriented tracheid with ends curved in a centrifugal direction; Figure 7D, 7E) or expansion; this orientation is demonstrated by P-type pitting whose scalariform patterning is perpendicular to the radial direction (Figure 7A-C, 7F-H). These anatomical features demonstrate the presence of a radially oriented polarity signal involved in the developmental regulation of the layer of radially aligned tracheids.

Together, these multiple lines of evidence demonstrate the presence of vascular cambial growth in *Perplexa*. The specific mode of secondary growth of this plant is characterized by an atypical radial component, represented by irregularly oriented tracheids and tracheid portions, and by a cambium that had unsychronized periclinal divisions. Anatomically, these features result in radial tracheid files with cells that are

irregular in size and shape (as seen in cross sections) and adjacent radial files that exhibit different numbers of tracheids, whose periclinal walls are offset radially.

Radial tissue systems and synchronization of periclinal divisions in Early Devonian euphyllophytes

To date, seven different plants from the Early Devonian have been demonstrated to possess secondary growth. Three of these are not as completely characterized (Gerrienne *et al.* 2011; Toledo *et al.* 2017; Gensel 2018). The four that have been formally described – *Armoricaphyton*, *Franhueberia*, G*mujij*, and *Perplexa* – allow us to consider the anatomical diversity of secondary xylem in the context of the evolution of vascular cambial growth regulation. For instance, these four plants exemplify several types of radial components in the anatomy of their secondary xylem. Some possess parenchymatous rays, thin (i.e., narrower than the tracheid files) and radially continuous, which are typically produced by asymmetrical periclinal divisions of cambial initials in extant seed plants. We see this type of rays in *Franhueberia* and *Armoricaphyton* (Table 3). In other cases, parenchymatous cells or series of cells replace tracheids in the radial files – as seen in G*mujij* and in some of the rays of *Armoricaphyton*. Because these cells have the same width as the tracheids that precede them centripetally in the file, I hypothesize that these radial structures were produced by a change in the fate of cambial derivatives in that cell file, i.e., from tracheid fate to parenchyma. Such a change in cell fate would involve a switch – associated with the periclinal (additive) cambial divisions – in the regulatory program responsible for cell differentiation. Moreover, some of these

parenchymatous files terminate abruptly, being replaced centrifugally by tracheids. This lends support to the hypothetical regulatory switch and suggests that the switch, if present, was reversible. Finally, the radial system organization of *Perplexa* (radially expanded tracheids and radially curved tracheid ends) adds another dimension to the range of structural features that reflect the presence of radial polarity in the regulatory mechanisms of secondary xylem development.

The four plants also exhibit differences in the tangential synchronization of periclinal divisions around their cambial layers. In *Armoricaphyton*, *Franhueberia*, and G*mujij*, adjacent tracheid files have the same numbers of tracheids, whose periclinal walls are tangentially aligned, reflecting well-synchronized periclinal divisions. In G*mujij* the tangential alignment of tracheids appears slightly offset in some places, but that is due to the lobed geometry of the primary xylem and the relatively reduced development of the secondary xylem around it. In contrast to the latter three plants, *Perplexa* features adjacent tracheid files with markedly different numbers of tracheids, whose periclinal walls are offset tangentially, reflecting a lack of tangential synchronization of cambial divisions.

Mosaic deployment of regulatory modules for secondary growth in Early Devonian euphyllophytes

These Early Devonian occurrences of woody plants reflect the modular nature of secondary growth regulation. On one hand, the four Early Devonian plants share several anatomical characters associated with cambial activity (Table 3), which suggest early-

evolved regulatory modules for secondary growth. On the other hand, these plants exemplify differences in anatomical characters associated with (1) the tangential synchronization of periclinal divisions of cambial initials, and (2) the production of a radial tissue system in the secondary xylem (Table 3). Such differences have implications for the modularity of some aspects of developmental regulation in vascular cambial growth.

Specifically, the anatomy of *Perplexa* indicates that tangential synchronization in cambial divisions is not required for the production of secondary tissues. This suggests that such synchronization is regulated independently from other aspects of vascular cambial growth. Considered together, the four plants also demonstrate that production of a radial tissue system can be achieved in different ways, with different regulatory mechanisms deployed independently or in combination. For instance, typical rays are produced by a module that determines asymmetric anticlinal divisions in cambial initials (e.g., *Franhueberia*). On the other hand, in G*mujij*, a reversible cell fate switch substitutes parenchyma cells for tracheids along radial tracheid files. Notably, *Armoricaphyton* demonstrates that these two modules can be deployed in concert (yet acting independently) in the same plant. Finally, *Perplexa* illustrates a type of radial system with no known parallels among living or extinct tracheophytes. While its anatomy demonstrates the presence of a radial polarity signal, the anatomical expression of this signal is less well defined and it is unclear what this implies from a regulatory standpoint. The distinct combinations of these characters in each plant (Table 3) reflect four different combinations of regulatory modules. In turn, these represent different modes of

secondary growth that are consistent with a mosaic pattern of assembly of these regulatory programs.

The anatomical characters shared among the four plants indicate several major components of vascular cambial growth that represent developmental modules, which had evolved by the Early Devonian: periclinal divisions of cambial initials, symmetric anticlinal divisions of cambial initials, and a radial polarity signal (Table 3). While a cambial layer that undergoes periclinal divisions is the *sine qua non* of cambial growth, addition of radial tracheid files by symmetric anticlinal divisions of cambial initials (multiplicative divisions) does not characterize the modes of secondary growth of all euphyllophytes. For instance, multiplicative divisions are not present in the secondary xylem of *Sphenophyllum* (Cichan & Taylor 1982), suggesting that the early-evolved regulatory module responsible for these divisions was lost or inactivated in the lineage. The presence of a radial tissue system in the secondary xylem of all four plants indicates that the differentiation of such a system within secondary tissues is a major aspect of vascular cambial growth that is regulated independently from, and upstream of, the modules responsible for the specific anatomy of the radial system (i.e., typical rays vs. radially oriented tracheids, etc.).

Equally important, the four Early Devonian plants had unifacial vascular cambia (i.e., none preserves evidence of secondary phloem), which have also been documented in other fossil lineages (e.g. sphenopsids, zygopterids; Cichan & Taylor 1990). Unifacial cambia are different from the vascular cambium of seed plants (and, more broadly, lignophytes), which is bifacial and produces both secondary xylem and secondary

phloem. The unifaciality of the cambium in multiple fossil lineages, including the earliest woody plants, may indicate that a regulatory module responsible for production of secondary tissues centrifugally from the cambium evolved later.

These broader considerations, along with the multiple modes of secondary growth illustrated by the Early Devonian fossils, indicate that vascular cambial growth is an assemblage of regulatory modules whose deployment followed a mosaic pattern in the evolution of tracheophytes (Tomescu & Groover 2019). As a result, while secondary growth is characterized across the board by a minimal set of developmental modules, which can be recognized by a corresponding set of structural fingerprints, different plants may not show all the traditional features that define tissues produced by vascular cambial growth. It is now becoming clear that vascular cambial growth encompassed a wide range of developmental modes by the Early Devonian. The diversity of modes of secondary growth and resulting anatomies present this early in the evolutionary history of euphyllophytes indicates that (1) the origins of this structural feature and of its modular components should be sought deeper in geologic time; and (2) that euphyllophytes were "experimenting" with different components of vascular cambial growth regulation exploring, in the process, the morphospace of secondary xylem anatomy. These different early woody plants may, indeed, represent ancestors of different younger euphyllophyte lineages known to possess secondary growth.

Conclusion

Perplexa praestigians gen. et sp. nov. is a significant addition to the growing diversity of anatomically preserved plants described from the Early Devonian, and is the newest member of a small group of Early Devonian euphyllophytes that shed light on the early evolution of cambial growth. Both the primary and the secondary xylem of this plant include features unlike those of any coeval plant, such as multiple mesarch peripheral protoxylem strands and a radial component of the secondary xylem consisting of radially expanded tracheids and tracheids with curved, radially oriented ends. In combination with the plesiomorphic *Psilophyton*-type tracheid pitting, these preclude the placement of *Perplexa* in any well-circumscribed euphyllophyte group. Furthermore, the superficial similarity of the primary xylem of *Perplexa* to that of the Early Devonian trimerophyte genus *Psilophyton* re-emphasizes the need for taxonomic re-evaluation of the latter. Comparative evaluation of *Perplexa* and the other well-characterized woody plants of the Early Devonian – *Armoricaphyton*, *Franhueberia*, and *Gmujij* – brings to light the breadth of anatomical diversity and complexity already present in secondary xylem at the time, and allows us to formulate hypotheses on the evolutionary assembly of regulatory programs responsible for specific anatomical features. Specifically, these Early Devonian plants demonstrate that vascular cambial growth exhibited a mosaic pattern of deployment of developmental regulatory modules. *Perplexa* and the other three plants each possess a unique combination of anatomical characters of secondary xylem,

reflecting different combinations of regulatory modules responsible for vascular cambial growth, which underpinned a diversity of modes of secondary growth during this period.

References

BANKS, H. P., LECLERCQ, S. and HUEBER, F. M. 1975. Anatomy and morphology of *Psilophyton dawsonii*, sp. n. from the Late Lower Devonian of Québec (Gaspe) and Ontario, Canada. *Palaeontographica Americana*, **8**, 75–127.

BECK, C. B. 1979. The primary vascular system of *Callixylon*. *Review of Palaeobotany and Palynology*, **28**, 103–115.

———. 1981. *Archeopteris* and its role in vascular plant evolution. *In* NIKLAS, K. J. (ed.) *Paleobotany, Paleoecology, and Evolution*, Praeger Publishers, New York, 193–230 pp.

BICKNER, M. A. and TOMESCU, A. M. F. 2019. Structurally complex, yet anatomically plesiomorphic: permineralized plants from the Emsian of Gaspé (Québec, Canada) expand the diversity of Early Devonian euphyllophytes. *IAWA Journal*, **40**, 421–445.

CANT, D. J. and WALKER, R. G. 1976. Development of a braided-fluvial facies model for the Devonian Battery Point Sandstone, Québec. *Canadian Journal of Earth Sciences*, **13**, 102–119.

CAVALIER-SMITH, T. 1998. A revised six-kingdom system of life. *Biological Reviews*, **73**, 203–266.

CICHAN, M. A. and TAYLOR, T. N. 1982. Vascular cambium development in *Sphenophyllum*: a Carboniferous arythrophyte. *IAWA Bulletin*, **3**, 155–160.

——— and ———. 1990. Evolution of cambium in geologic time - a reappraisal. *In*

IQBAL, M. (ed.) *The Vascular Cambium*, Research Studies Press LTD., Somerset, England, 213–229 pp.

DENNIS, R. L. 1974. Studies of Paleozoic ferns: *Zygopteris* from the Middle and Late Pennsylvanian of the United States. *Palaeontographica. Abteilung B*, **148**, 95–136.

EGGERT, D. A. 1961. The ontogeny of Carboniferous arborescent Lycopsida. *Palaeontographica. Abteilung B*, **108**, 43–92.

GENSEL, P. G. 2018. Early Devonian woody plants and implications for the early evolution of vascular cambia. *In* KRINGS, M., HARPER, C., CUNEO, N. R. and ROTHWELL, G. W. (eds.) *Transformative Paleobotany*, Vol. 1. Academic Press, London, 21–33 pp.

GERRIENNE, P. and GENSEL, P. G. 2016. New data about anatomy, branching, and inferred growth patterns in the Early Devonian plant *Armoricaphyton chateaupannense*, Montjean-sur-Loire, France. *Review of Palaeobotany and Palynology*, **224**, 38–53.

———, ———, STRULLU-DERRIEN, C., LARDEUX, H., STEEMANS, P. and PRESTIANNI, C. 2011. A simple type of wood in two Early Devonian plants. *Science*, **333**, 837.

GRIFFING, D. H., BRIDGE, J. S. and HOTTON, C. L. 2000. Coastal-fluvial palaeoenvironments and plant palaeoecology of the Lower Devonian (Emsian), Gaspé Bay, Québec, Canada. *In* FRIEND, P. and BPJ, W. (eds.) *New Perspectives on the Old Red Sandstone*, Vol. 180. Geological Society, London, 61–84 pp.

HARTMAN, C. M. and BANKS, H. P. 1980. Pitting in *Psilophyton dawsonii*, an Early Devonian trimerophyte. *American Journal of Botany*, **67**, 400–412.

HOFFMAN, L. A. and TOMESCU, A. M. F. 2013. An early origin of secondary growth: *Franhueberia gerriennei* gen. et sp. nov. from the Lower Devonian of Gaspé (Québec, Canada). *American Journal of Botany*, **100**, 754–763.

JOY, K. W., WILLIS, A. J. and LACEY, W. S. 1956. A rapid cellulose peel technique in palaeobotany. *Annals of Botany*, **20**, 635–637.

KENRICK, P. and CRANE, P. R. 1997. *The origin and early diversification of land plants*. Smithsonian Institution Press, Washington and London.

MATSUNAGA, K. K. S., STOCKEY, R. A. and TOMESCU, A. M. F. 2013. *Honeggeriella complexa* gen. et sp. nov., a heteromerous lichen from the Lower Cretaceous of Vancouver Island (British Columbia, Canada). *American Journal of Botany*, **100**, 450–459.

NIKLAS, K. J. and CREPET, W. L. 2020. Morphological (and not anatomical or reproductive) features define early vascular plant phylogenetic relationships. *American Journal of Botany*, **107**, 1–12.

PFEILER, K. C. and TOMESCU, A. M. F. In review. An Early Devonian actinostelic euphyllophyte with secondary growth from the Emsian of Gaspé (Canada) and the importance of tracheid wall thickening patterns in early euphyllophyte systematics. *Palaeontology*.

R CORE TEAM. 2018. R: A language and environment for statistical computing.

STRULLU-DERRIEN, C., KENRICK, P., TAFFOREAU, P., COCHARD, H.,

BONNEMAIN, J. L., LE HÉRISSÉ, A., LARDEUX, H. and BADEL, E. 2014. The earliest wood and its hydraulic properties documented in c. 407-million-year-old fossils using synchrotron microtomography. *Botanical Journal of the Linnean Society*, **175**, 423–437.

SZERAKOWSKA, S., SULEWSKA, M. J., TRZCIŃSKI, J. and WORONKO, B. 2015. Comparison of methods determining the angularity of aggregate particles. *Applied Mechanics and Materials*, **797**, 246–252.

TOLEDO, S. 2018. A new anatomically-preserved plant form the Lower Devonian of Québec (Canada): implications for euphyllophyte phylogeny and early evolution of structural complexity. MSc thesis. Humboldt State University, 1–101pp.

———, BIPPUS, A. C. and TOMESCU, A. M. F. 2017. Early hints of structural complexity: a new euphyllophyte from the Lower Devonian of Québec. Botanical Society of America conference abstract. Available at: http://2017.botanyconference.org/engine/search/index.php?func=detail&aid=119.

———, ——— and ———. 2018. Buried deep beyond the veil of extinction: euphyllophyte relationships at the base of the spermatophyte clade. *American Journal of Botany*, **105**, 1–22.

TOMESCU, A. M. F. and GROOVER, A. T. 2019. Mosaic modularity: an updated perspective and research agenda for the evolution of vascular cambial growth. *New Phytologist*, **222**, 1719–1735.

TOMIZONO, S. 2013. boxplotdbl: Double box plot for two-axes correlation.

TRANT, C. A. and GENSEL, P. G. 1985. Branching in *Psilophyton*: a new species from

the Lower Devonian of New Brunswick, Canada. *American Journal of Botany*, **72**, 1256–1273.

Tables

Table 1. Summary statistics for comparisons of metaxylem tracheid widths (μm)

	Perplexa	*Psilophyton*	*Archaeopteris*	*Zygopteris*
Average	31.1	38.7	55.2	52.3
Median	31.0	38.1	55.9	53.7
Min	9.0	25.2	26.3	14.8
Max	60.0	64.9	92.9	89.7
n	91	20	31	30

Table 2. Summary statistics for comparisons of secondary xylem tracheid radial and tangential widths (µm).

Radial widths

	Perplexa	*"Psilophyton"*	*Archaeopteris*	*Zygopteris*
Average	50.5	53.1	33.3	98.4
Median	51.5	52.8	32.0	89.6
Min	23.0	26.5	22.5	46.1
Max	72.0	122.4	47.7	228.7
n	46	47	28	80

Tangential widths

	Perplexa	*"Psilophyton"*	*Archaeopteris*	*Zygopteris*
Average	29.1	33.3	28.1	78.5
Median	29.0	31.5	29.5	72.6
Min	11.0	16.0	10.9	29.5
Max	42.0	53.0	41.4	187.5
n	56	47	28	80

Table 3. Mosaic expression of anatomical fingerprints and corresponding developmental processes or hypothesized regulatory modules controlling vascular cambial growth in Early Devonian euphyllophytes.

Anatomical character *Regulatory module for ~*	*Perplexa*	*Sagaweigmujij*	*Armoricaphyton*	*Franhueberia*
Radially aligned tracheid files *Periclinal divisions of cambial initials*	X	X	X	X
Tangentially aligned tracheids *Synchronization of periclinal divisions*		X	X	X
Multiplicative divisions of tracheid files *Symmetrical anticlinal divisions of cambial initials*	X	X	X	X
Radial system *Radial polarity signal/gradient*	X	X	X	X
Radially oriented tracheids/tracheid parts *Directionality of cell expansion*	X			
Parenchyma replacing tracheids in radial files (irregular rays) *Cell fate switch in cambial derivatives*		X	X	
Typical parenchymatous rays *Asymmetric anticlinal divisions of cambial initials*			X	X

Figures

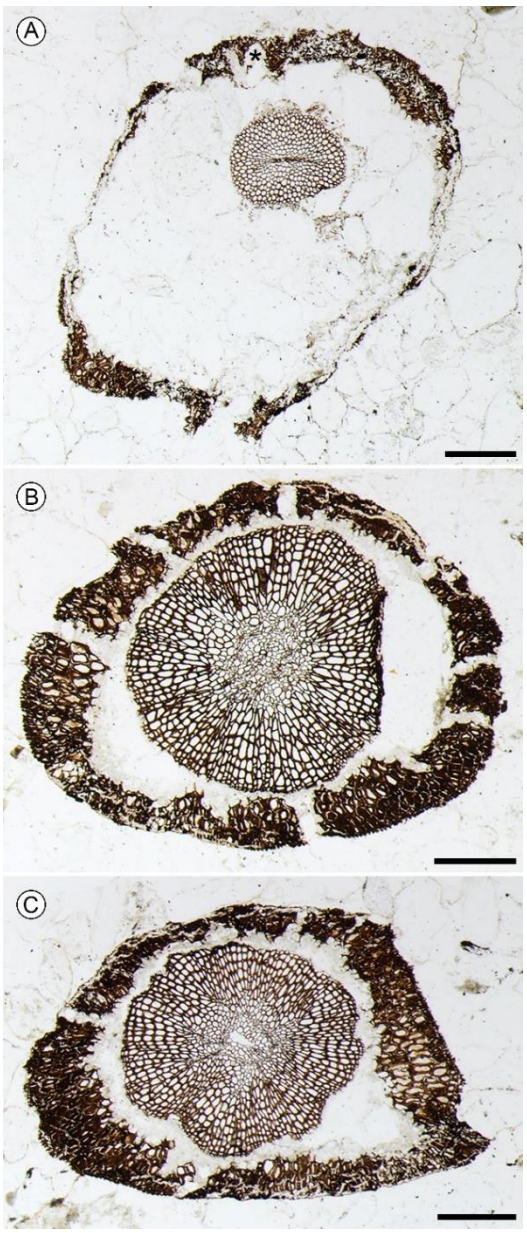

Figure 1. ***Perplexa praestigians*** **gen. et sp. nov.** axis anatomy in cross section. **A**, distal-most axis portion; central cylinder of primary xylem, wide inner cortex (not preserved), thin, sclerified, incompletely preserved outer cortex with substomatal chamber (asterisk), secondary growth absent. USNM 557820-4 Bbot #10a. **B**, Basal portion of axis; lightly lobed central primary xylem, thick layer of secondary xylem, thin

inner cortex (not preserved), thick sclerified outer cortex with gaps representing substomatal chambers. USNM 557820-4 Cbot #1a. **C**, Basal-most portion of axis, tissue layering same as in B. USNM 557820-4 D #5a. Scale bars = 500 µm.

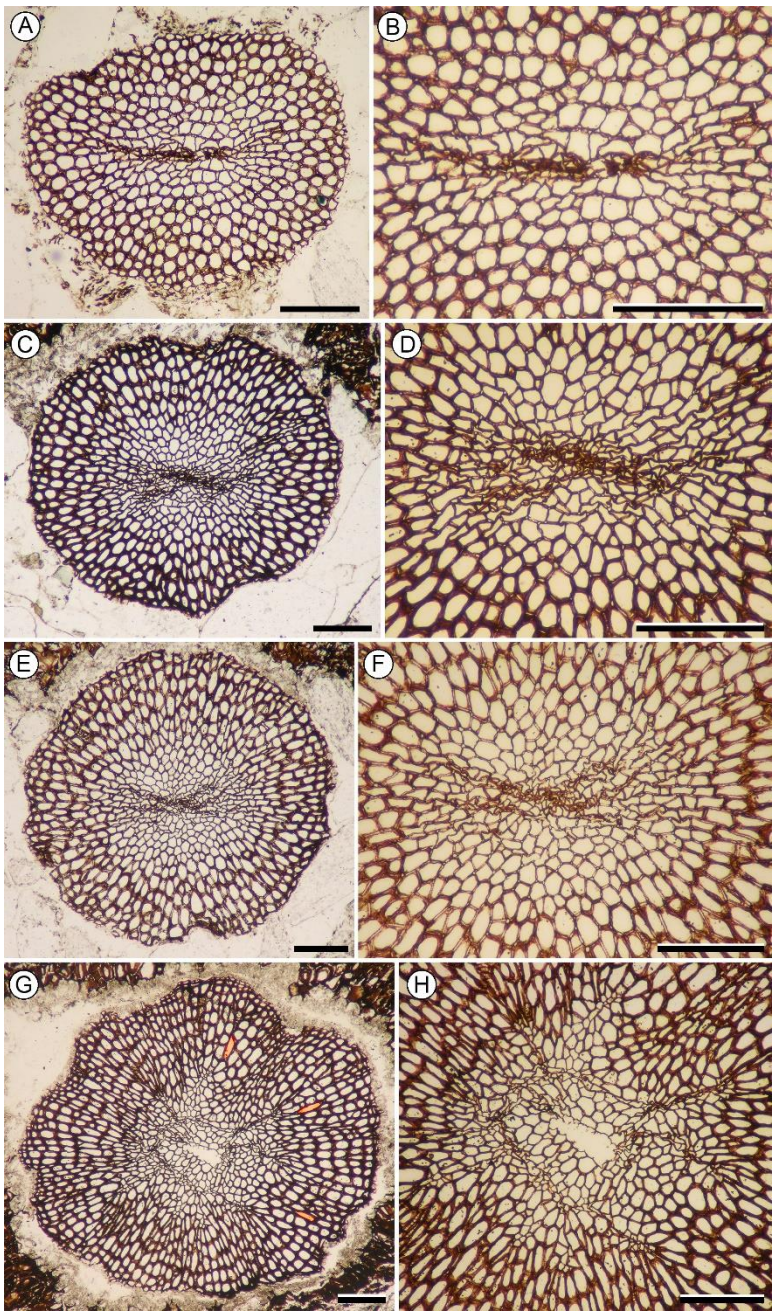

Figure 2. ***Perplexa praestigians*** **gen. et sp. nov.** xylem anatomy in cross section from the basal portion (bottom) to the distal portion (top) of the axis. **A**, **B**, Distal-most potion of axis lacking secondary growth and with two mesarch areas of protoxylem in diametrically opposite locations; compressed central region of metaxylem has the appearance of centrach xylem maturation. USNM 557820-4 Bbot #10d. **C**, **D**, Distal region of the axis portion with secondary xylem; note thin layer of secondary xylem,

crushed central metaxylem, three or four mesarch protoxylem strands (D), and narrow, radially elongated cell in secondary xylem at 2 o'clock in C. USNM 557820-4 Cbot #215a. **E**, **F**, Distal region of the axis portion with secondary xylem; note crushed central metaxylem, four mesarch protoxylem strands (F), and radially oriented tracheid in secondary xylem at 10 o'clock in E. USNM 557820-4 Cbot #163a. **G**, **H**, Basal-most portion of axis showing clear mesarch xylem maturation and secondary growth; note the different numbers of tracheids per file and the radially offset periclinal walls in adjacent tracheid files; tracheids highlighted in red are twice as wide radially as adjacent tracheids (refer to Figure 6F for longitudinal radial section). USNM 557820-4 D #5a. Scale bars = 200 µm.

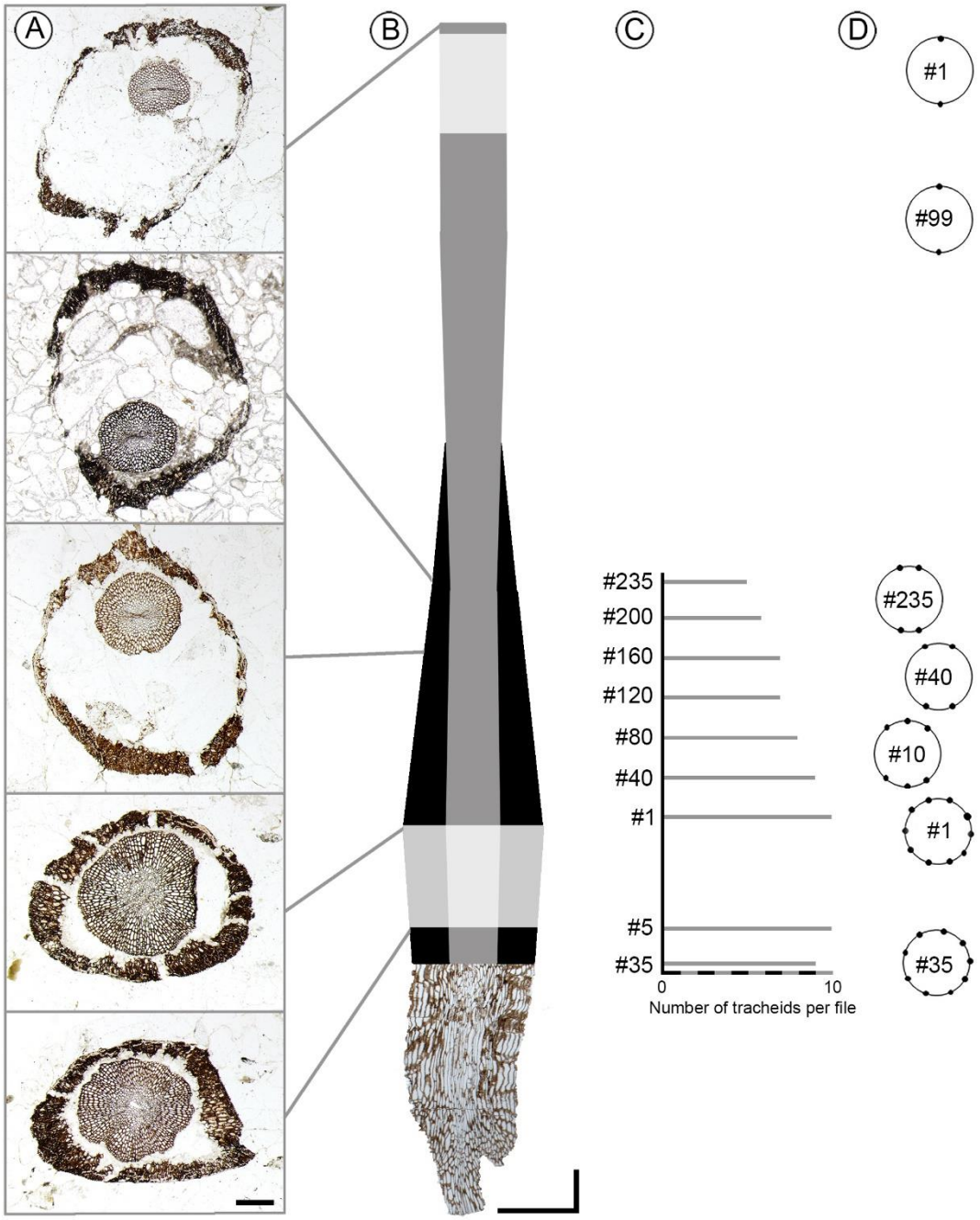

Figure 3. ***Perplexa praestigians*** **gen. et sp. nov.** anatomical variation along the axis. **A**, Cross sections of entire axis (see caption of Figure 1); note proximo-distal trends of increasing axis diameter, inner cortex width, and (minimally) primary xylem thickness; and decreasing outer cortex and secondary xylem thickness; sections from top to bottom: USNM 557820-4 Bbot #10d, Cbot #235a, Cbot #163a, Cbot #1a, D#5a. Scale bar = 500

μm. **B**, Reconstruction of metaxylem (gray) diameter and secondary xylem (black) thickness along the axis; white regions indicate saw cuts (~2.5 mm) between cobble slabs USNM 557820-4 D (bottom), USNM 557820-4 C (middle), and USNM 557820-4 B (top). Longitudinal radial section of basal-most axis portion (USNM 557820-4 D2S #113a) at the same scale, at base of panel; note thinner-walled tracheids at center. Horizontal and vertical scale bars = 1 mm; horizontal exaggeration x2. **C**, Thickness of secondary xylem represented as maximum numbers of tracheids per radial file; vertical axis (with peel numbers) at same scale and vertically aligned with diagram in B. **D**, Proximo-distal decrease in number and change in relative positioning of protoxylem poles (dots) along axis, as illustrated by selected sections (peel numbers at center of circles); circles are just for reference and do not represent the outline of the primary xylem; diagrams vertically aligned with the position of the corresponding sections in B. Note protoxylem poles forming two groups with diametrically opposite locations.

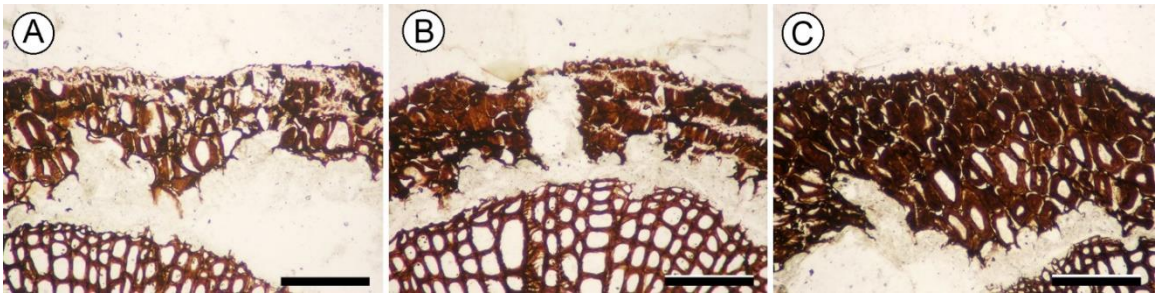

Figure 4. ***Perplexa praestigians*** **gen. et sp. nov.** epidermis and sclerified outer cortex in cross section. **A**, Small epidermal cells (left) bounded by laterally continuous putative cuticle. **B**, Distorted epidermal cells (center-right) and substomatal chamber in outer cortex (center). **C**, Abraded epidermis with anticlinal cell walls protruding from axis surface. Note thick secondary walls of outer cortex cells. USNM 557820-4 Cbot #1a. Scale bars = 200 µm.

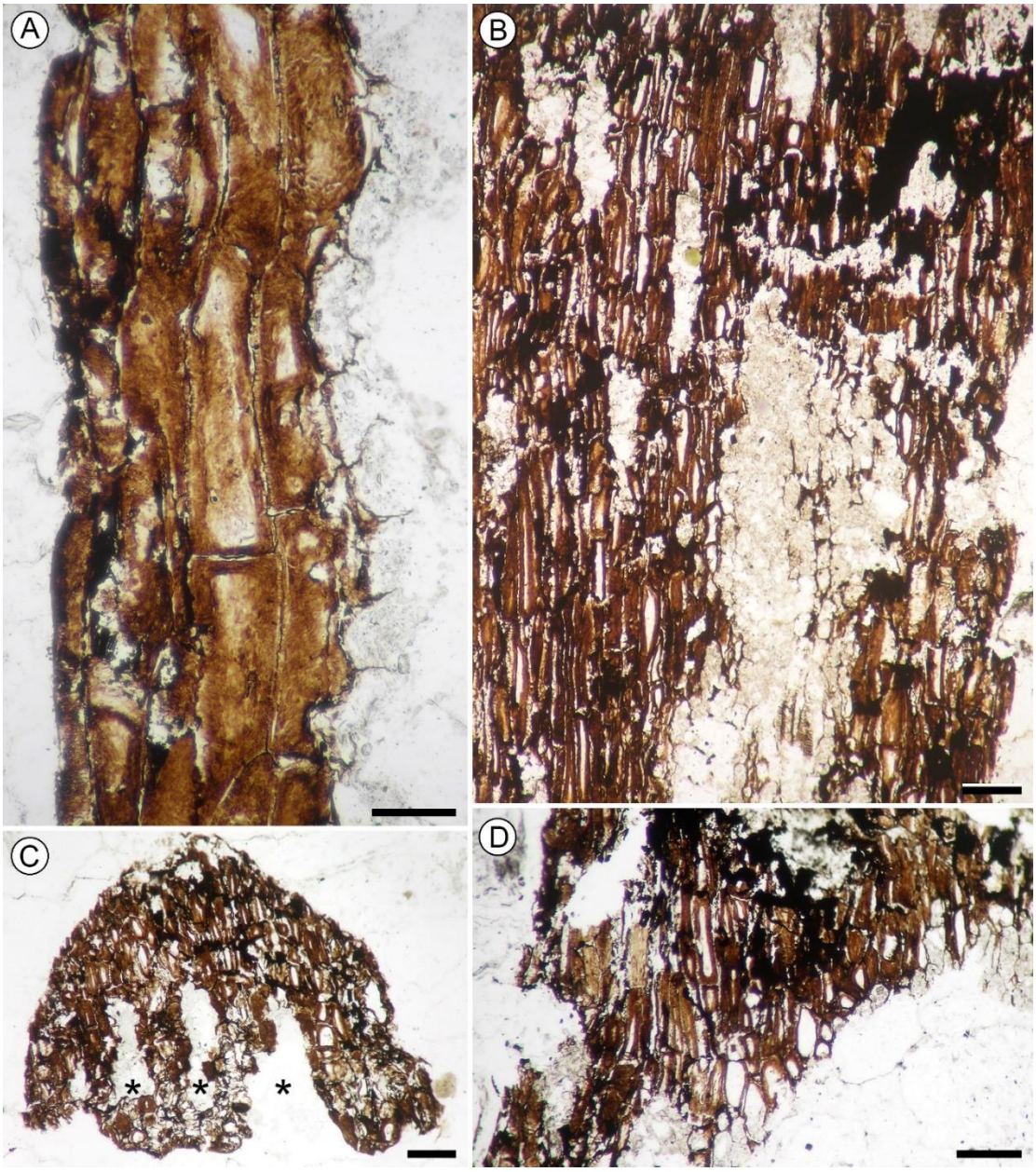

Figure 5. ***Perplexa praestigians* gen. et sp. nov.** longitudinal sections of sclerified outer cortex and inner cortical cells in longitudinal section. **A**, Detail of sharp transition from the sclerified outer cortex to the parenchymatous inner cortex (right); note thick secondary walls of outer cortex cells and remnants of the thin horizontal anticlinal walls of inner cortex cells adjacent to the outer cortex. USNM 557820-4 D2S #111a. Scale bar = 100 µm. **B**, Longitudinal tangential section of outer and inner cortex; note vertical, columnar outer cortex cells and shorter, oval parenchyma of the inner cortex (center). USNM 557820-4 D2S #169a, scale bar = 200 µm. **C**, Longitudinal tangential section of

outer cortex with elongated vertical gaps of three substomatal chambers (asterisks; one chamber incompletely sectioned at right); note regular arrangement of substomatal chambers. USNM 557820-4 D2S #4a, scale bar = 200 µm. **D**, Oblique longitudinal tangential section of outer cortex with columnar cells and incompletely parenchyma of inner cortex adjacent to the outer cortex. USNM 557820-4 D2S #13a, scale bar = 200 µm.

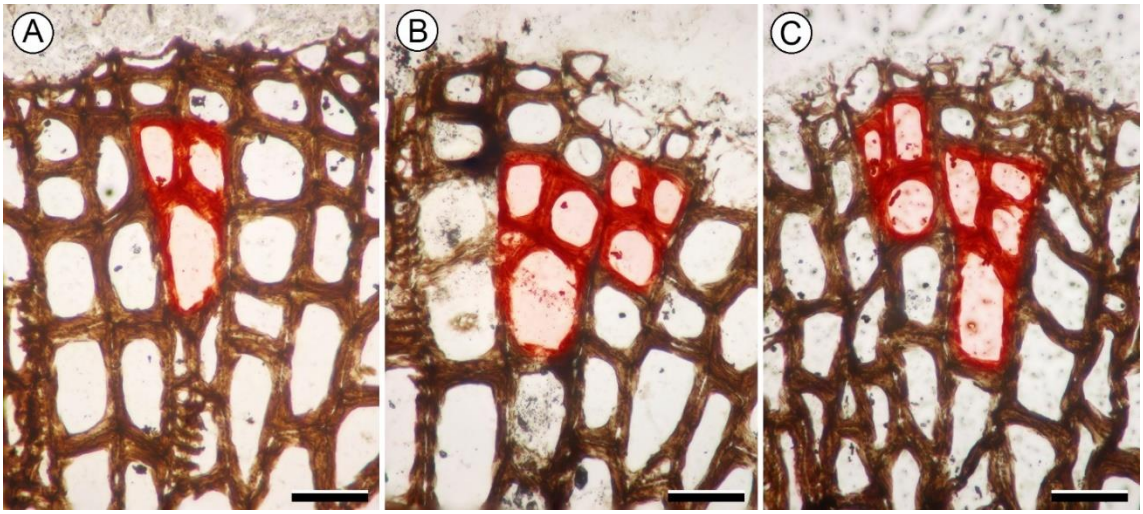

Figure 6. ***Perplexa praestigians*** **gen. et sp. nov**. multiplicative divisions in the secondary xylem (in red). Note tracheids in penultimate position within radial files with smaller radial widths and fully developed, thick secondary walls; outermost tracheids with thinner walls (sometimes missing outer periclinal walls); radially oriented tracheid (left in B). **A**, USNM 557820-4 Cbot #20a. **B**, **C**, USNM 557820-4 Cbot #25a. Scale bars = 50 μm.

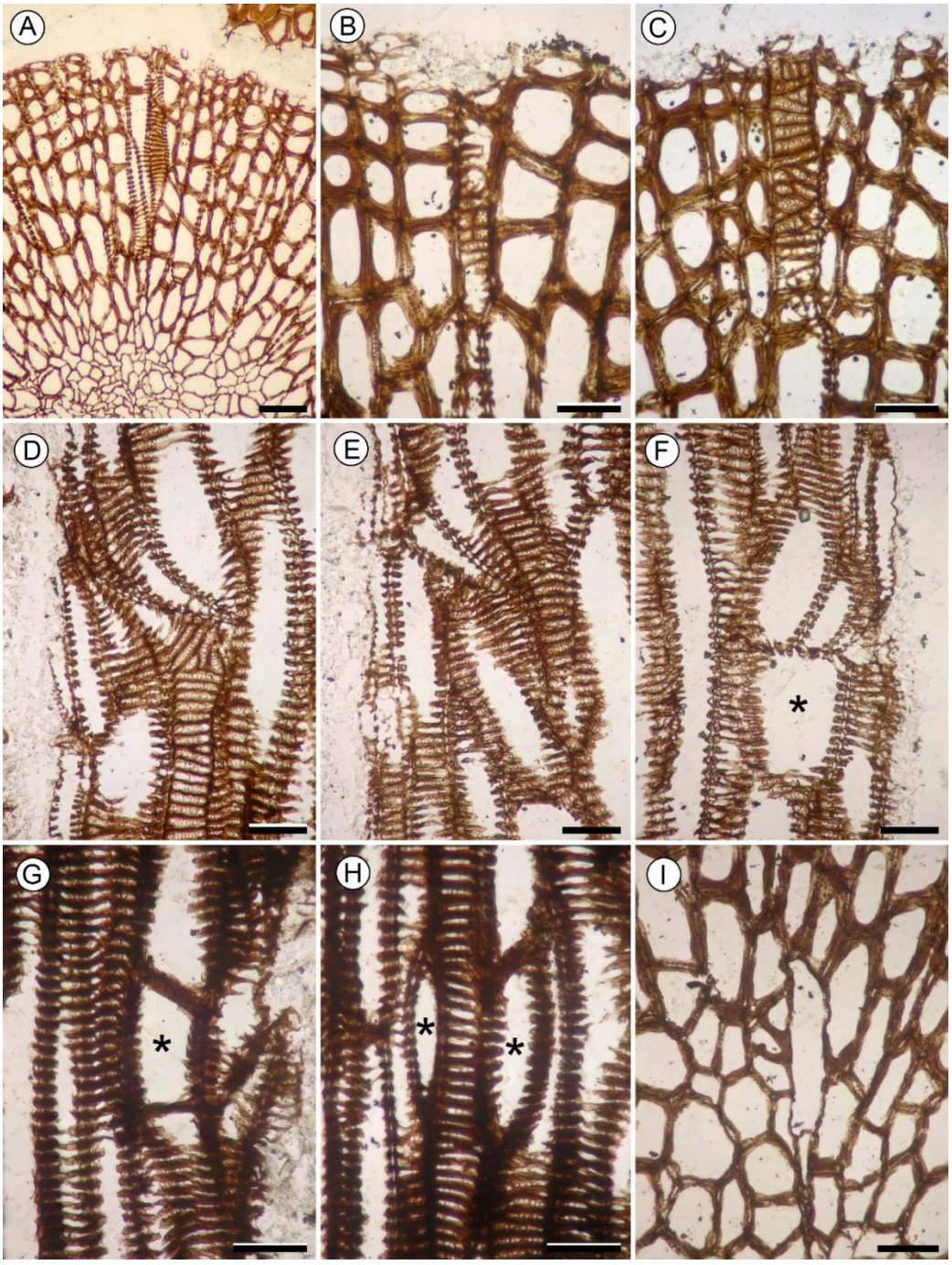

Figure 7. ***Perplexa praestigians*** **gen. et sp. nov.** radial component of secondary xylem. **A**, **B**, **C**, Tracheids with radial orientation demonstrated by orientation of their *Psilophyton*-type pitting (as seen in cross section); note tracheids in penultimate position within radial files with smaller radial widths and fully developed secondary walls; outermost tracheids with thinner walls (sometimes missing outer periclinal walls). A:

USNM 557820-4 Cbot #5a, scale bar = 100 µm; B: USNM 557820-4 Cbot #25a, scale bar = 50 µm; C: USNM 557820-4 Cbot #5a, scale bar = 50 µm. **D**, **E**, Longitudinal radial sections of tracheids with sharply curved and radially oriented ends; note uniseriate apertures of the *Psilophyton*-type thickenings. USNM 557820-4 D2S #80a. Scale bars = 50 µm. **F**, Longitudinal radial section of tracheid (asterisk) that is short and twice as wide as those vertically adjacent. USNM 557820-4 D2S #80a. Scale bar = 50 µm. **G**, **H**, Longitudinal tangential sections of tracheids (asterisks) that are short and entirely (G) or partially (H) oriented radially (as indicated by the orientation of their *Psilophyton*-type thickenings); these may represent radially oriented tracheid ends. G: USNM 557820-4 D2S #54a; H: USNM 557820-4 D2S #50a; scale bars = 50 µm. **I**, Radially elongated cell devoid of secondary wall thickenings (seen in cross section), located at the transition between metaxylem and secondary xylem. USNM 557820-4 Cbot #2a. Scale bar = 50 µm.

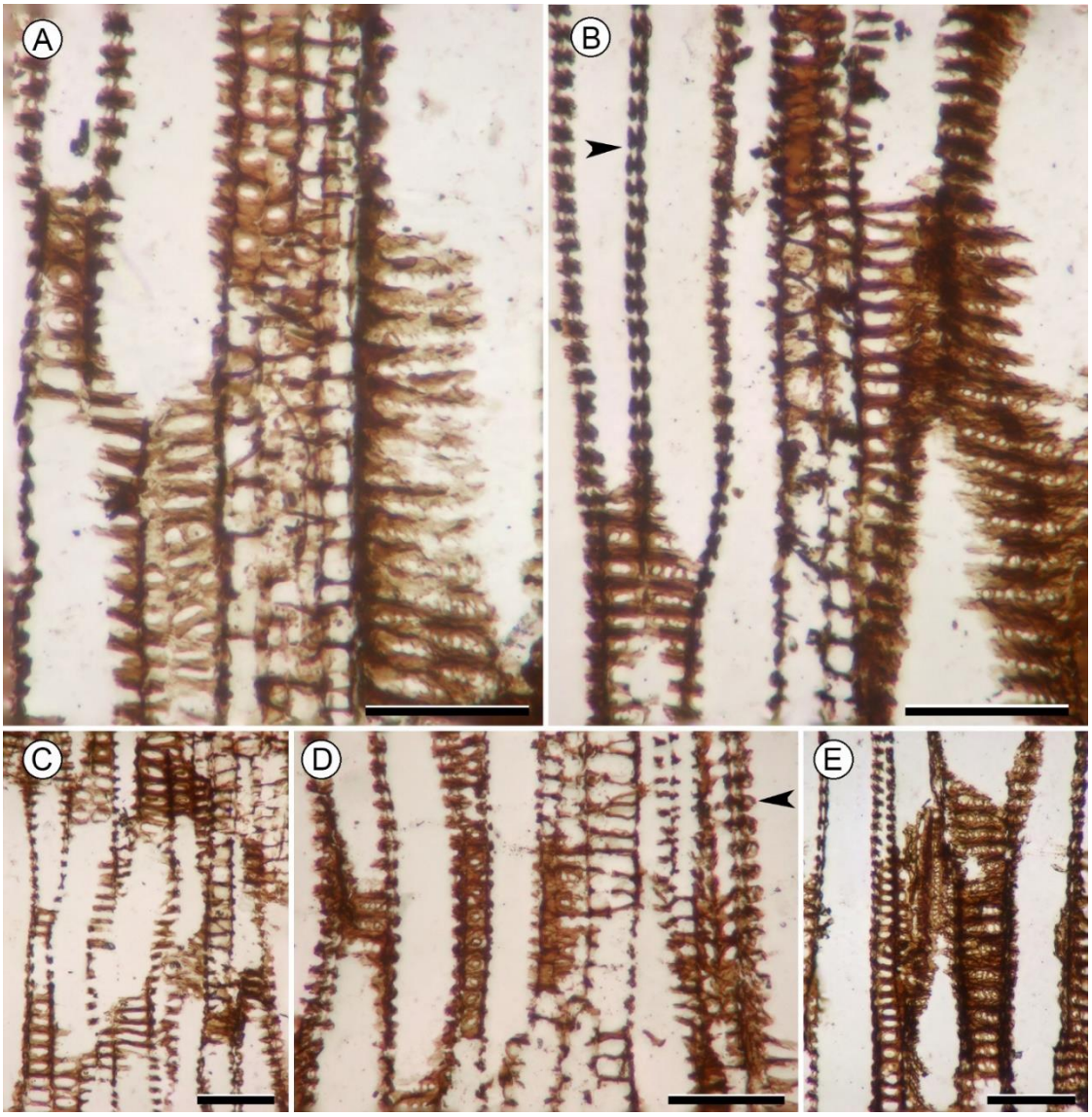

Figure 8. ***Perplexa praestigians*** **gen. et sp. nov.** primary xylem anatomy in longitudinal section. **A**, Protoxylem tracheids with annular thickenings (center); note narrow metaxylem tracheids with uniseriate bordered pits (left and center-top) and with horizontal oval bordered pits (bottom left). USNM 557820-4 D2S #85a. **B**, Protoxylem tracheids with annular thickenings (center bottom); *Psilophyton*-type thickenings with one oval or two circular apertures (bottom left), oval bordered pits transitioning to a scalariform pattern (right of protoxylem), and pit pairs with shallow thickenings and narrow combined pit chambers (arrowhead). USNM 557820-4 D2S #85a. **C**, Metaxylem tracheids with thin scalariform thickenings (right) and horizontal oval bordered pits (center and left). USNM 557820-4 D2S #80a. **D**, Metaxylem tracheids with thin scalariform thickenings (center right) and uniseriate bordered pits (center left);

arrowhead indicates tracheids with the scalariform bars of *Psilophyton*-type thickenings protruding markedly into the cell lumen and deep-set pit membranes. USNM 557820-4 D2S #80a. **E**, Metaxylem tracheids with horizontal oval bordered pits (left) and with typical *Psilophyton*-type pitting (center right) transitioning to pits with 2-3 apertures (bottom); note top end of tracheid at center with the *Psilophyton*-type pitting pattern intriguingly oriented parallel with (and not perpendicular to) the longitudinal axis of the tracheid. USNM D2S 557820-4 D2S #85a. Scale bars = 50 µm.

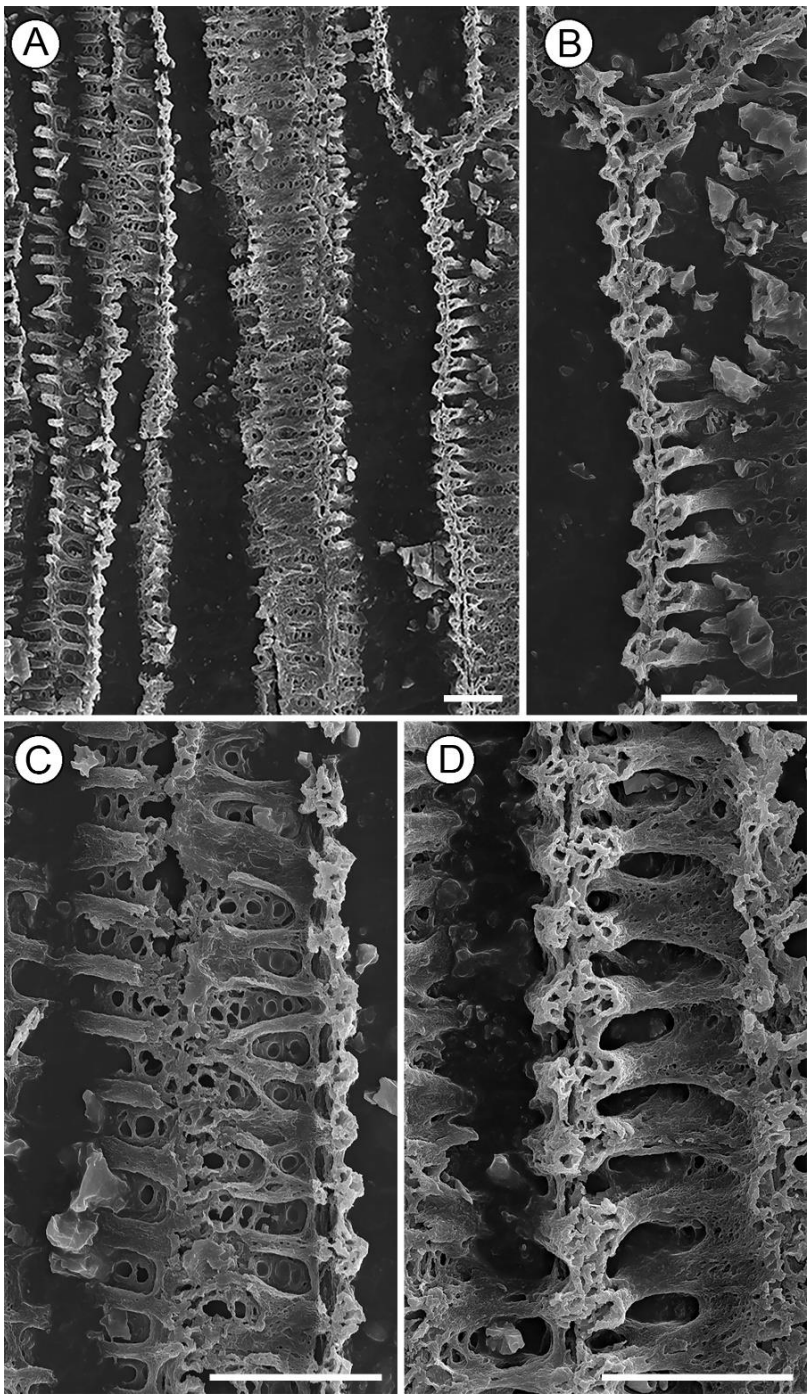

Figure 9. ***Perplexa praestigians*** **gen. et sp. nov.** longitudinal views of tracheid anatomy in scanning electron microscopy. Note typical *Psilophyton*-type thickenings (A-D); some thickenings have three, two, or one aperture in the membrane (bottom left in A); irregularly shaped pits (right in C); narrow, slit-shaped pit pair chambers (B-D);

scalariform bars of the *Psilophyton*-type pitting protruding more (B, D) or less (C) into the cell lumen; overall spongy internal structure of the scalariform bars of *Psilophyton*-type pitting. B and C are details of A. USNM D2S #77. Scale bars = 25 µm.

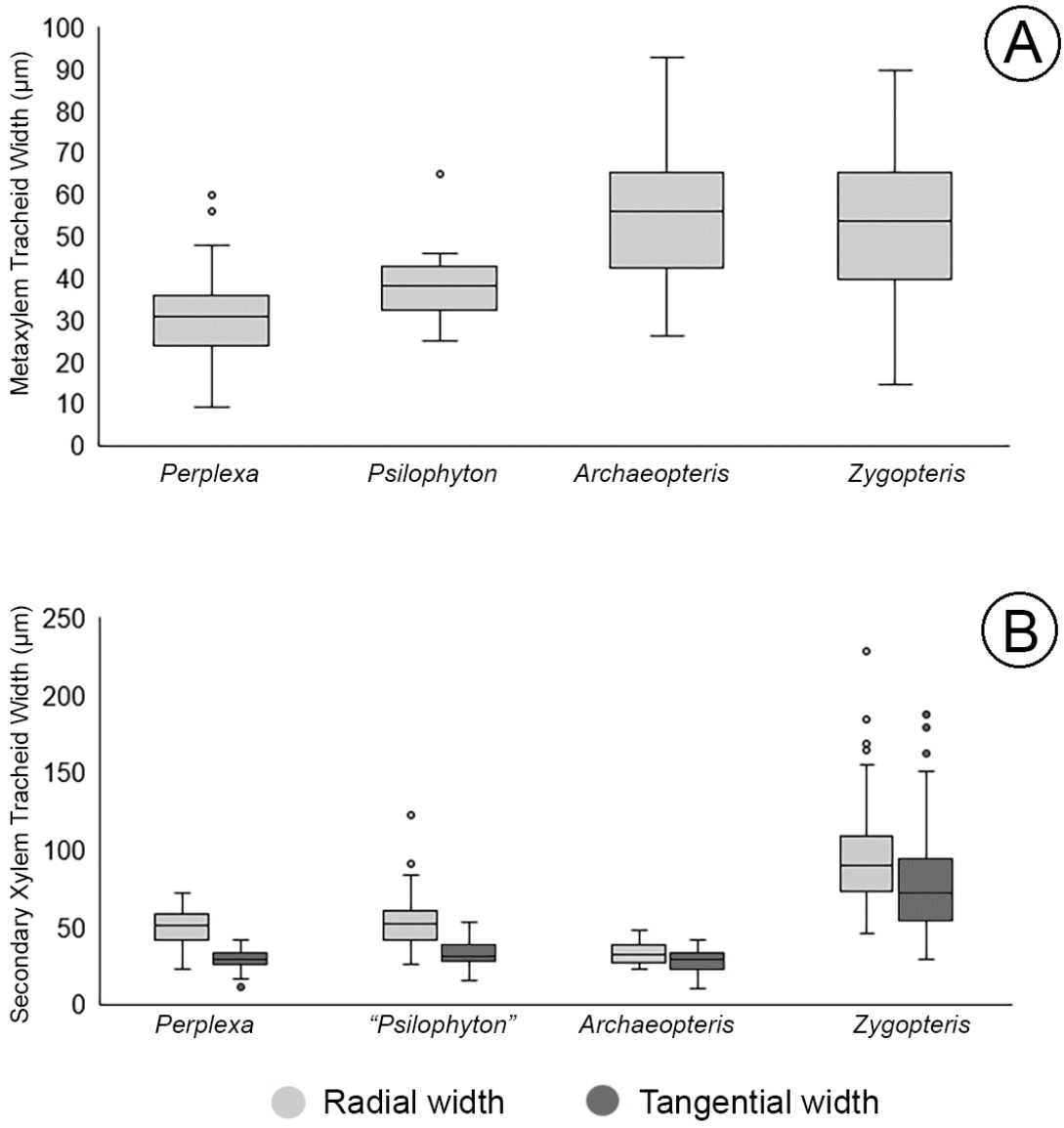

Figure 10. Comparisons of metaxylem (A) and secondary xylem (B) tracheid widths (see Material and Methods for sources of measurements and Tables 1 and 2 for summary statistics; see Comparisons – Tracheid Sizes for "*Psilophyton*" label in B). Boxes represent interquartile ranges with medians as horizontal bars; whiskers represent the first and third quartile; circles represent outliers.

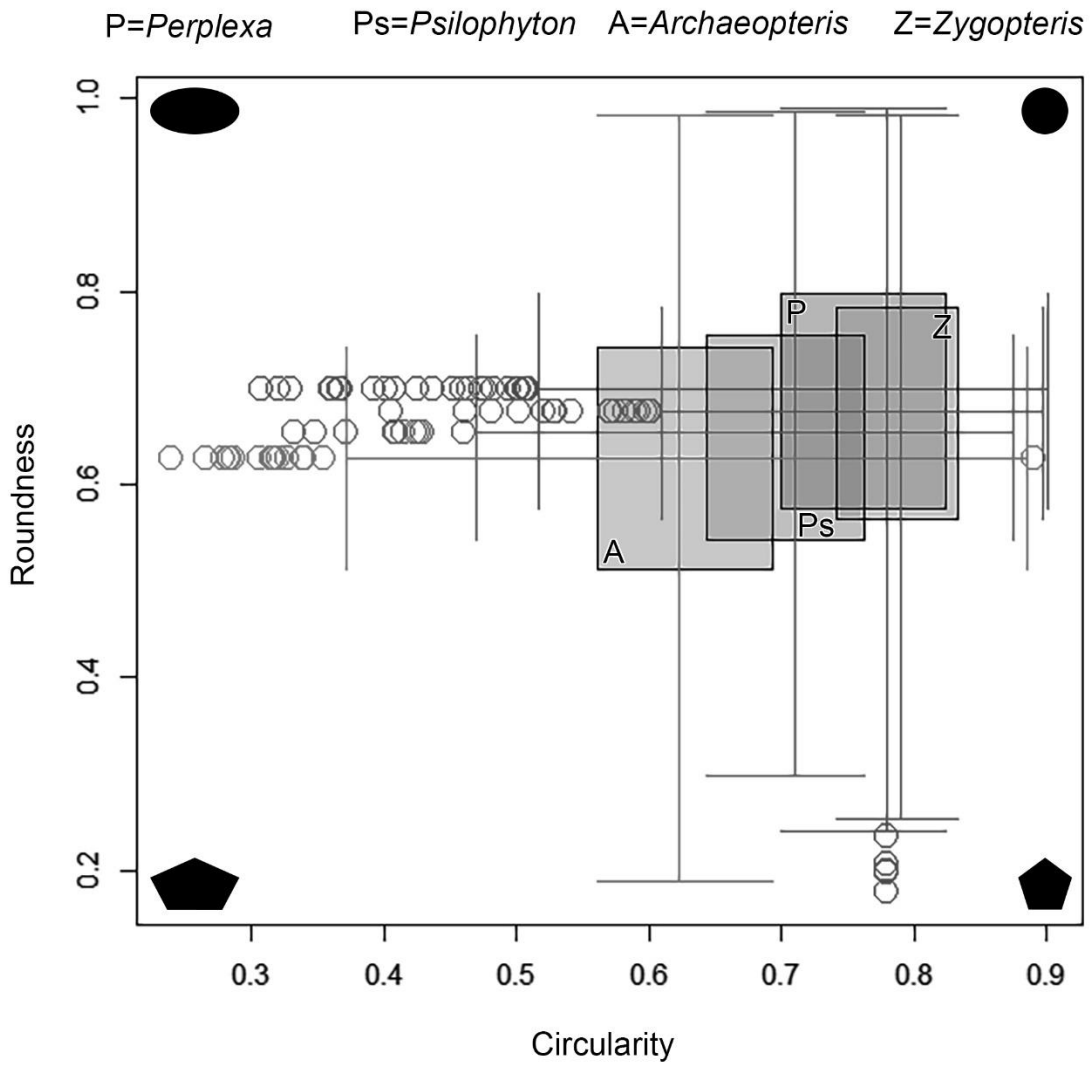

Figure 11. Comparisons of roundness and circularity of metaxylem tracheids (see Material and Methods for sources of measurements). Boxes represent interquartile ranges with medians as horizontal and vertical bars; whiskers represent the first and third quartile; circles represent outliers.